Naval Research Laboratory

Washington, DC 20375-5320

NRL/FR-MM/5710--05-10,097

Development of a Vertically Launched Decoy Vehicle

MICHAEL J. VERACKA
ALVIN CROSS

Offboard Countermeasures Branch
Tactical Electronic Warfare Division

CARLOS FIGUEROA

ITT Industries, Advanced Engineering & Sciences
Alexandria, VA 22303

August 31, 2005

REPORT DOCUMENTATION PAGE

Form Approved
OMB No. 0704-0188

1. REPORT DATE *(DD-MM-YYYY)*	**2. REPORT TYPE**	**3. DATES COVERED** *(From - To)*
31-08-2005	Formal Report	September 1998 - June 2005

4. TITLE AND SUBTITLE

Development of a Vertically Launched Decoy Vehicle

5a. CONTRACT NUMBER

5b. GRANT NUMBER

5c. PROGRAM ELEMENT NUMBER
62270N

6. AUTHOR(S)

Michael J. Veracka, Alvin Cross, and Carlos Figueroa*

5d. PROJECT NUMBER

5e. TASK NUMBER
EW-70-1-02

5f. WORK UNIT NUMBER
6136

7. PERFORMING ORGANIZATION NAME(S) AND ADDRESS(ES)

Naval Research Laboratory
4555 Overlook Ave., SW
Washington, DC 20375

8. PERFORMING ORGANIZATION REPORT NUMBER

NRL/FR-MM/5710--05-10,097

9. SPONSORING / MONITORING AGENCY NAME(S) AND ADDRESS(ES)

Office of Naval Research
875 North Randolph Street
Arlington, VA 22203

10. SPONSOR / MONITOR'S ACRONYM(S)

ONR

11. SPONSOR / MONITOR'S REPORT NUMBER(S)

12. DISTRIBUTION / AVAILABILITY STATEMENT

Approved for public release; distribution is unlimited.

13. SUPPLEMENTARY NOTES

*ITT Industries, Advanced Engineering & Sciences, Alexandria, VA 22303

14. ABSTRACT

Advanced infrared imaging missiles pose a formidable threat to U.S. Navy ships operating in the littorals. Advanced materials and techniques for accurately placing them will be necessary to counter these threats. This report describes the development of a decoy vehicle compatible with the next generation of naval ships, which will have decoy launchers below deck to minimize their radar signature. This vehicle is launched vertically and pitches over to fly horizontally in any direction. It has a large central payload cavity suitable for carrying a variety of decoy and obscurant materials.

15. SUBJECT TERMS

IR countermeasures
Expendables
Imaging IR decoy
Obscurants
Vertically launched decoy

16. SECURITY CLASSIFICATION OF:			**17. LIMITATION OF ABSTRACT**	**18. NUMBER OF PAGES**	**19a. NAME OF RESPONSIBLE PERSON**
a. REPORT	**b. ABSTRACT**	**c. THIS PAGE**			Michael J. Veracka
Unclassified	Unclassified	Unclassified	UL	37	**19b. TELEPHONE NUMBER** *(include area code)* (202) 767-1302

Standard Form 298 (Rev. 8-98)
Prescribed by ANSI Std. Z39.18

CONTENTS

EXECUTIVE SUMMARY E1

1. INTRODUCTION 1

2. DEMONSTRATION VEHICLE GOALS AND CONSTRAINTS 2

   2.1 Mission Constraints 3
   2.2 Practical Constraints 3

3. CONCEPTUAL DESIGN — MAJOR SUBSYSTEMS 3

   3.1 Airframe 4
   3.2 Gas Flight Control System 5
   3.3 Flight Computer 6
   3.4 Parachute Recovery System 6

4. CONCEPT STUDY AND PARAMETRIC DESIGN 7

   4.1 Initial Study Results and Revisions 8
   4.2 VLIIRDT Parametric Study 8

5. DETAILED DESIGN 12

   5.1 General Construction and Fasteners 12
   5.2 Nose Subassembly and GFCS 12
   5.3 Fuselage Section 14
   5.4 Aft Subassembly 14
   5.5 Flight Computer 16

6. MANUFACTURING, ASSEMBLY, AND INTEGRATION 17

   6.1 GFCS Manufacturing and Assembly 17
   6.2 Airframe Manufacturing and Assembly 18
   6.3 Flight Computer Packaging and Assembly 19
   6.4 Vehicle Integration 19
   6.5 Additional Subsystems 20

7. VEHICLE TESTING 21

   7.1 Preflight Testing 21
   7.2 Flight Testing 22

8. CONCLUSIONS 28

9. RECOMMENDATIONS 29

BIBLIOGRAPHY 30

APPENDIX A — September 25, 2002 Flight Test Data Plots 31

APPENDIX B — May 1, 2003 Flight Test Data Plots 33

EXECUTIVE SUMMARY

Advances in infrared imaging (IIR) arrays and microprocessors are placing new demands on decoys to counter the improved tracking and target discrimination capabilities of the IIR threats. To be effective, decoy and obscurant materials will have to be placed properly. Additionally, future naval ships will have most of their equipment below deck to minimize visual, infrared, and radar signatures. The Vertically Launched Imaging Infrared Decoy Technologies (VLIIRDT) effort was a 6.2 initiative to develop the technologies necessary to counter advanced threats to naval surface platforms. This report provides the details on the design, fabrication, and testing of the VLIIRDT decoy vehicle.

Under ONR sponsorship, the VLIIRDT effort demonstrated a decoy vehicle designed to be compatible with the next generation of naval ships. As seen in the pictures, the VLIIRDT decoy vehicle is launched vertically then pitches over and flies horizontally. The vehicle employs an innovative steering mechanism contained in the nose of the vehicle that uses cold gas thrust to provide full attitude control (pitch, yaw, and roll). Servomotors connected to ball valves controlled the gas thrusters that steer the vehicle. The thrust for the vehicle's forward flight is provided by a single-stage rocket motor housed in the tail section. The combination of these two systems resulted in a vehicle that has a large central payload cavity suitable for carrying and deploying decoy material.

Click here to view movie

DEVELOPMENT OF A VERTICALLY LAUNCHED DECOY VEHICLE

1. INTRODUCTION

Advances in imaging infrared (IIR) arrays and microprocessors are placing new demands on decoys to counter the improved tracking and target discrimination capabilities of the IIR threats. The Vertically Launched Imaging Infrared Decoy Technologies (VLIIRDT) effort was a 6.2 initiative to develop the technologies necessary to counter these advanced threats to naval surface platforms. The technologies addressed under the 6.2 effort included

- obscurant materials to reduce the IR signature of the "protected" platform,
- low-visible, spectrally balanced radiative materials to provide a false target, and
- a vertically launched vehicle to carry the IR payloads.

This report provides the details on the design, fabrication, and testing of the VLIIRDT vehicle. The work to develop obscurant and radiative payload materials will be covered in a separate report.

Figure 1 shows a functional concept for the VLIIRDT effort. Vertically deployed decoys provide the mechanism for controlling cloud placement and establishing the pattern of IR clouds. In this functional scenario, the deployment heading for the decoys is passed to an autopilot immediately prior to launch of the decoys and is selected to optimize effectiveness. The decoys are rocket launched vertically from the launcher, then pitchover to a level horizontal flight away from the ship. Upon reaching a level horizontal flight, the decoys begin to sequentially dispense the payloads during their flight profile. The obscurant clouds are deployed forward of the ship, and the radiative materials are deployed aft. As the decoys are deployed from the launcher, the ship steams forward, behind the obscurant clouds, so that the only IR target in the threat field-of-view is the IR-emitting "false target" clouds. The threat then tracks the false target as the ship is masked by the obscurant materials.

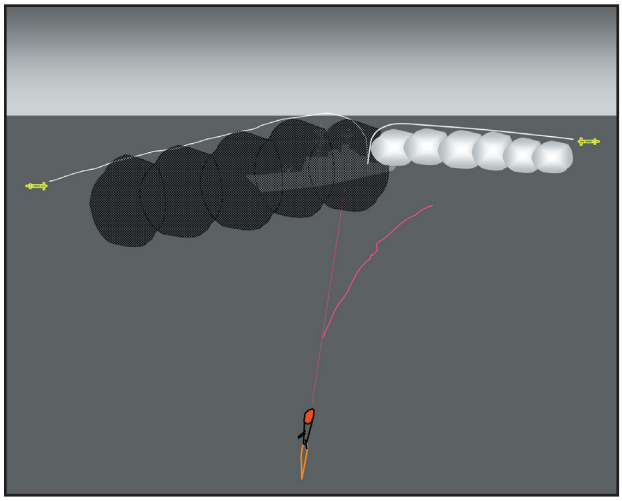

Fig. 1 — VLIIRDT functional concept

Manuscript approved June 26, 2005.

Development of a vertically launched vehicle to deploy the decoy payload materials was addressed in this effort. It offered several advantages over traditional decoy designs that are compatible with the MK-36 launcher and are typically used on U.S. Navy platforms. First, a vertical launch decoy system is compatible with low signature requirements for future naval platforms. Secondly, deploying the decoy vertically provides an "all-aspect" capability, meaning that one decoy system can be responsive to any threat direction. Thus, this effort addressed the development of a decoy that could be stowed beneath the ship deck, launched vertically, and programmed to fly a flight profile in any direction. This report discusses the effort to develop a vehicle capable of achieving a horizontal flight profile after a vertical launch.

2. DEMONSTRATION VEHICLE GOALS AND CONSTRAINTS

The demonstration vehicle was designed based on the following mission goals:

- Vertical launch — vehicle will be stowed below the deck of future naval ships
- Flight altitude below 150 ft — material cloud must be between the ship and the threats that fly near the water surface
- Fly 1,400 ft downrange — provide the ability to dispense materials anywhere along the distance covered by a ship moving at 20 knots for 30 s
- Maintain heading within ±10 deg — accurate placement of material is essential
- Hold roll attitude within ±20 deg — payload is dispensed downward

A study was conducted in 1999 to determine the feasibility of such a vehicle. The payload weight and flight range were established based on the amount and placement of material that would be needed to be an effective decoy for a surface combatant ship. A launcher was selected, which limited the outer dimensions of the vehicle. From these constraints, the size of control surfaces necessary to ensure enough maneuverability was determined. A six-degree-of-freedom (6-DOF) model was used to simulate the vehicle dynamics in accomplishing the mission goals within the known constraints. The results of this model were then used to design the vehicle.

The initial design of the vehicle consisted of two canards on the front of the vehicle to provide the aerodynamic control. This design would allow control of the vehicle while reducing complexity by using a few moving surfaces. A minimum airspeed was required for the canards to function effectively. To achieve this airspeed, the use of a dual stage rocket motor is indicated: a first thrust to lift the vehicle vertically and provide the necessary airspeed for the canards to steer the vehicle and a second thrust to propel the vehicle forward after it has pitched over and pointed in the desired direction of flight. By using two stages, the vehicle could accomplish the pitchover at the lower height that is critical for the effective placement of the decoy material. However, a motor of this type would be unique to this application and would be cost-prohibitive even in production quantities. To keep the vehicle as inexpensive as possible, a second design was proposed and modeled.

The second design used a gas-thrust vector control steering mechanism. The 6-DOF simulation confirmed that the vehicle could be controlled using cold gas thrusters. Six thrusters arranged around the perimeter of the nose of the vehicle could provide all of the control necessary to allow the pitchover maneuver and guide the vehicle along the desired flight path. An additional benefit of this design is that the gas thrusters were capable of steering the vehicle at much slower airspeeds than control surfaces. By using gas thrusters for steering, a simpler and less expensive one-stage rocket motor could be used to propel the vehicle. The gas thruster method appeared to be simpler, more robust, and less expensive than using control surfaces to guide the vehicle.

2.1 Mission Constraints

Figure 2 shows the type of flight profile the VLIIRDT vehicle would have to fly to perform its mission. This flight profile was the primary factor in determining the performance specifications and design characteristics of the demonstration vehicle.

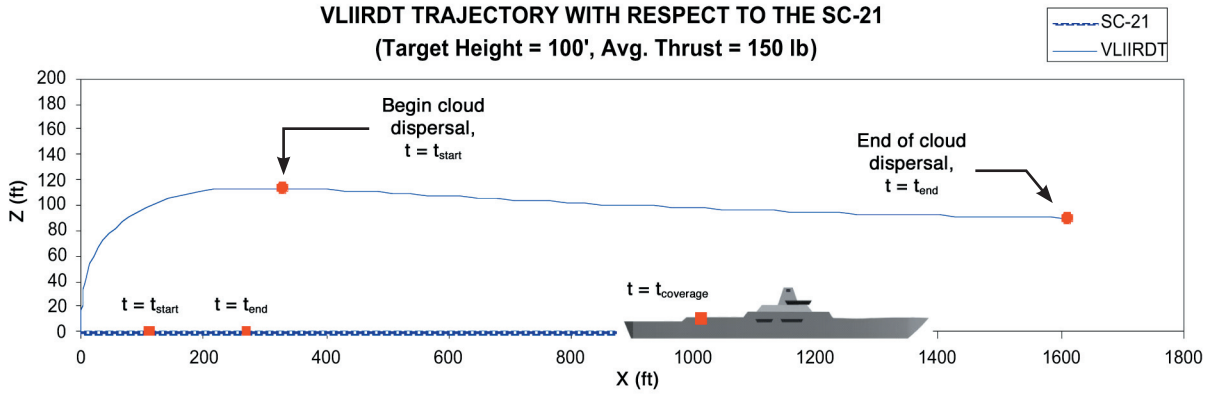

Fig. 2 — VLIIRDT flight profile

The vertical launch deployment, pitchover, and 1,400-ft horizontal flight path distance could be achieved more easily using rocket propulsion instead of the more common mortar launch. The use of deployable fins to provide aerodynamic stability once the vehicle was in flight was selected to meet storage requirements.

The mission requirement that the vehicle fly at altitudes less than 150 ft above ground level placed additional constraints on the design. Achieving the low-altitude flight profile requires the vehicle to execute a 90-deg turn to a near-horizontal flight path. Aerodynamic controls were considered, but making these surfaces both deployable and controllable is very complicated. Aerodynamic surfaces also require significant airspeed to be effective. This required speed would make it difficult to make a sharp turn. A nonaerodynamic control system, such as compressed gas thrusters, could control the vehicle at any speed and is more effective at the slower speeds after launch. An array of six nozzles around the perimeter of the nose of the vehicle would provide full attitude control with no external moving parts.

2.2 Practical Constraints

The demonstration vehicle dimensions were set to a 9 in. by 9 in. cross section because the decoy was intended to be demonstrated using the base of an MK-53 launcher that currently deploys Nulka decoys. The length of the vehicle was determined to be 75 in. by considering the amount of space needed to store the vehicle components and the amount of payload that vehicle would be expected to carry. To reduce development time and cost, many parts and system components in the vehicle were commercially available off-the-shelf items. A parachute recovery system was used to enable repeated use of the test vehicle.

3. CONCEPTUAL DESIGN — MAJOR SUBSYSTEMS

The component layout shown in Fig. 3 was conceived as a starting point for the design. In this design, the entire control system is housed in the nose of the vehicle. The deployable fins and the rocket motor are both at the rear of the vehicle. This provides a very large volume of approximately 60 liters available for the payload. In addition, the only moving parts in the vehicle are the fins and the solenoid valves that control the gas flow.

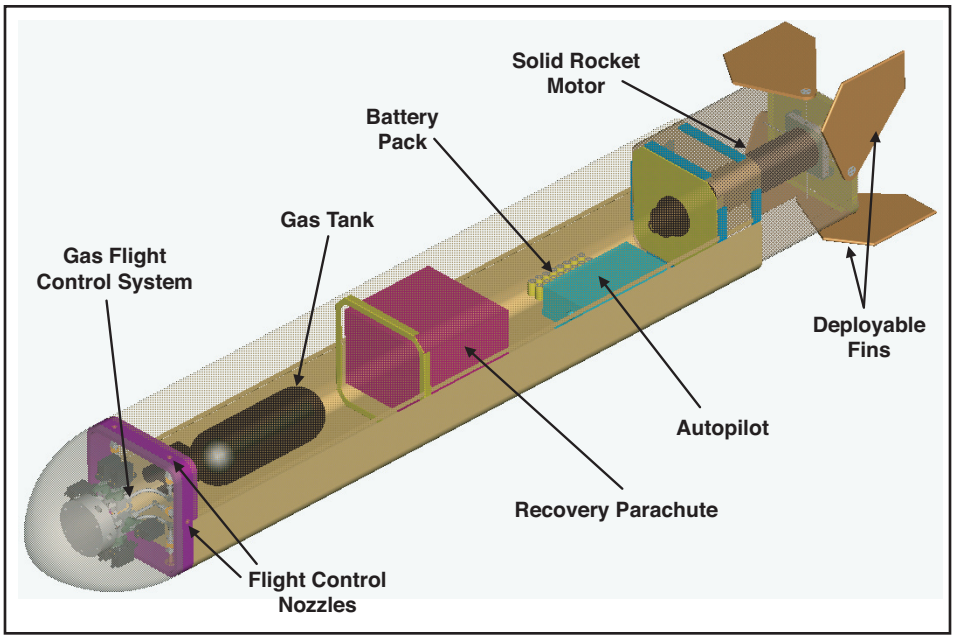

Fig. 3 — Initial component layout

3.1 Airframe

The VLIIRDT forward airframe section consists of two U-shaped halves made of aluminum and joined with screws and rivets. A separate aft fuselage section that contains the tail fin assembly and the rocket motor mount is attached. The square-bodied vehicle is manufactured and assembled using thin sheet metal structures with reinforcing bulkheads to achieve high strength with fairly low weight and cost.

The bottom half of the fuselage serves as the permanent base to which all of the components are attached. The top half is a cover, which is attached after access to the inner components is no longer needed during testing of the demonstration vehicle. Primarily, this access hatch is utilized to provide quick access for changing the battery and filling the gas bottle.

Thin reinforcing bulkheads are distributed along the fuselage to give structural rigidity to help the thin sheets retain their shape. At the nose, the bulkhead that contains the gas-thruster nozzles is the major structural component of the vehicle. This forward bulkhead is also the support for the entire Gas Flight Control System (GFCS) and its attachment to the vehicle, as well as a hard point for the recovery parachute attachment. The other structural hard point for the parachute is the interface between the main and aft fuselage sections. This part of the vehicle is very sturdy, since this is where the tail's aerodynamic loads and the rocket propulsion forces interact with the vehicle.

Four tail fins are deployed from the aft section of the vehicle and are mounted on the outside of the aft section. This section has a smaller cross section than the rest of the vehicle so that the fins are flush with the payload section of the vehicle in its stowed configuration. Upon deployment, the fins automatically pivot from the side of the body into the air stream as the vehicle exits the launch tube. They were sized according to computer modeling and wind tunnel experimentation to achieve the desired stability margin.*

*Andrea B. Walden, AISLE Six-Degree-of-Freedom Concept Study, April 1999.

3.2 Gas Flight Control System

As shown in Fig. 4, the GFCS controls the flight of the vehicle by receiving commands from the flight computer and actuating valves to release compressed gas through nozzles. The GFCS consists of a high-pressure storage tank and regulator that feeds a manifold for distribution to the six nozzles through separate valves.

The vehicle's six nozzles provide full 3-axis control for the vehicle—two nozzles for independent yaw control and four nozzles for coupled pitch and roll control. Figure 5 shows the arrangement of the nozzles around the nose of the vehicle, and the associated table shows the nozzles that are activated to achieve the desired results.

Proportional valves were chosen to give more precise control of the gas flow, and thus, the vehicle. By using a high-torque/high-speed servomotor, the valves would provide proportional control up to the maximum nozzle thrust available for the given reservoir pressure. Commercial radio control (R/C) servos are widely available and easily interface to the valves of the GFCS.

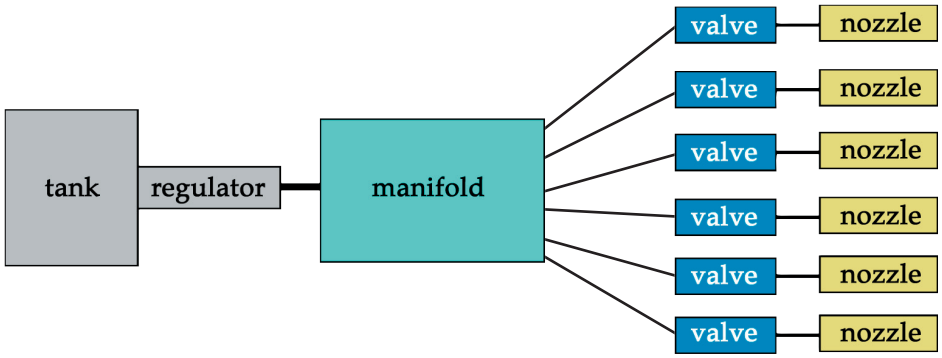

Fig. 4 — VLIIRDT GFCS diagram

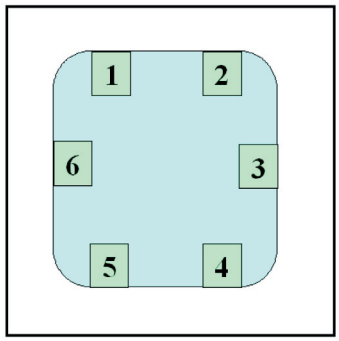

	Up	Down
Pitch	4 + 5	1 + 2
	Left	Right
Roll	1 + 4	2 + 5
Yaw	3	6

Fig. 5 — VLIIRDT GFCS nozzle control scheme (seen from rear)

3.3 Flight Computer

A flight computer is used to log aerodynamic data, the pilot's servo commands, and the vehicle's response to those commands during flight. The following flight data items were collected for post-flight analyses:

- Inertial state of the vehicle (3 body-axis accelerations and rotation rates)
- Air data (airspeed, angle of attack (α), sideslip angle (β), and static pressure)
- GFCS servo commands
- Global Positioning System (GPS) (latitude, longitude, altitude, ground track, climb rate, and ground speed)

This information is recorded from the Inertial Measurement Unit (IMU), various pressure transducers, a pulse width modulation (PWM) timer card, and GPS receiver. The information is stored on board at high resolution and also sent in a lower resolution to the ground station computer via a wireless modem to insure data capture if the vehicle was unexpectedly damaged during flight or recovery. The goal is to compare the actual results with original estimates from the simulation results and refine the simulation to make it more accurate and aid in the development of an autopilot. Figure 6 shows a diagram of the system components.

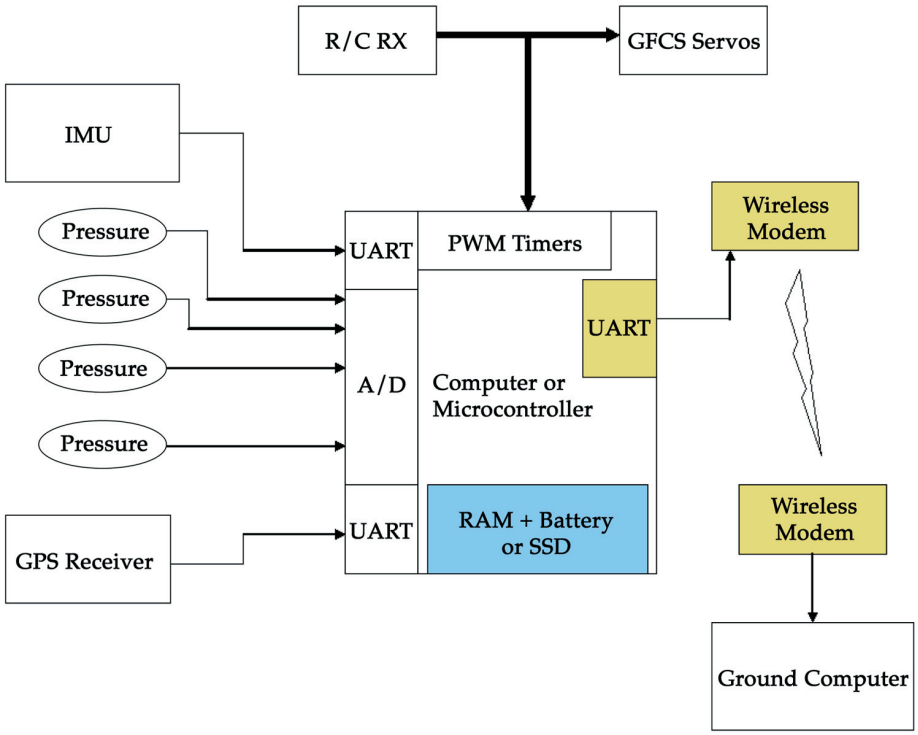

Fig. 6 — Flight computer system

Table 1 shows the required bandwidth to transmit these data for each of the components. The wireless modem requires 9 bits per byte sent. A 4,050 bytes per second bandwidth is needed for this wireless communication. A modem transmission rate of 38,400 bits per second, which delivers 4,266 bytes per second of bandwidth, satisfies the data transmission requirements.

3.4 Parachute Recovery System

A parachute that allows a safe descent is used so that the vehicle can be tested multiple times. The parachute is deployed through the top of the vehicle through a hatch that is remotely actuated. The parachute slows the vehicle to a descent rate of less than 10 ft/s for safe recovery.

Table 1 — Flight Computer Components Data Bandwidths

Component	Amount	Update Rate (Hz)	Data Size (bytes)	Data Rate (bytes per second)
IMU	1	100	12	1200
A/D channel	5	30	2	300
PWM channel	6	50	2	600
GPS message	1	5	300	1500
			Total Data Rate	3600

The harness that connects the vehicle to the parachute is attached to the vehicle at four points to minimize any rocking motion during descent and to reduce damage at impact. The lengths of the straps are arranged to allow the vehicle to descend in a slight nose-up orientation to protect the GFCS components in the nose upon landing. The only expected damage after a flight is a broken tail fin if the parachute inflates late and fails to slow the vehicle's descent rate enough to land softly. Figure 7 shows the vehicle descending after a flight with the parachute fully deployed.

Fig. 7 — Vehicle descending with the parachute deployed

4. CONCEPT STUDY AND PARAMETRIC DESIGN

In the initial phase of the VLIIRDT program, a study was conducted to verify the feasibility of the preliminary vehicle design and its capability to achieve the required mission flight profile. The study included a flight simulation using a feedback loop autopilot. The following parameters were varied during the course of the study:

- Vehicle weight and center-of-gravity
- GFCS nozzle thrust
- GFCS volume
- GFCS servo frequency

The results narrowed the choices to a combination of parameters that served as starting points for the vehicle design and allowed a subscale wind tunnel model to be constructed to refine the design. The wind tunnel testing results were then incorporated into a computer simulation to further refine the design.

4.1 Initial Study Results and Revisions

Results from the study provided performance estimates for GFCS reservoir sizing, actuator specification, nozzle design, and weight budgeting. The study determined that 5 lb of thrust per nozzle was adequate to control the vehicle in flight. Both carbon dioxide and nitrogen were considered as working gases. The amount of gas required with carbon dioxide was lower than that of nitrogen since it has more mass per unit volume. However, nitrogen was selected because integrated tank/regulator assemblies for nitrogen containment and delivery were available off-the-shelf from the paintball industry. The stability criterion of a 2-in. static margin was verified and used to narrow the center-of-gravity (CG) location. The study showed that servo response needed to be faster than 5 Hz to effectively stabilize the vehicle. Based on the load limit of the launching system, the initial weight budget was set to 80 lb.

Two aspects of the vehicle simulated in the study were changed in the current VLIIRDT vehicle. The initial vehicle design was assumed to require a two-phase boost, where the first booster would eject the vehicle out of the launcher to the desired flight altitude and power the pitchover maneuver. The second booster would power the remainder of the vehicle flight in the chosen direction. By modifying the design to use gas to control the vehicle instead of control surfaces, this two-stage burner could be replaced with a single booster. This decreased the cost and increased the reliability by using a simpler propulsion system that eliminated the need to eject the first booster stage and ignite the second after pitching over. Single-stage rocket boosters are available off-the-shelf and could accomplish the proper flight profile because of the GFCS.

Another change was the configuration of the GFCS nozzles. The original vehicle design used four nozzles for yaw, two on each side, and two for pitch, one each on the top and bottom. This was reversed to four in pitch and two in yaw because pitch was the most critical maneuvering axis for the desired flight profile. Both nozzle configurations yielded identical roll control.

4.2 VLIIRDT Parametric Study

The results obtained from the study fixed the length of the vehicle and helped define the component layout. This was followed by a more detailed study of the vehicle's aerodynamic characteristics and the specifications of some of the components. The aerodynamic characteristics, the weight, and mass distribution were measured. The results of these measurements were then incorporated into the simulation to refine the detailed design.

4.2.1 Wind Tunnel Testing

Using the results from the computer simulations, a half-scale wind tunnel model was constructed to obtain the vehicle's aerodynamic characteristics. Additionally, the wind tunnel model provided data used to select the body corner radius and span of the tail fins (based on a 2-in. static margin stability). In the simulation, the fin span was varied while the root chord was set to 8 in. and the tip chord was set to 6 in. for the full-scale vehicle. As shown in Fig. 8, the geometry selected for the half-scale model was a span of 3 in. and a body corner radius of 10 percent of the body's dimension.

The wind tunnel model provided a full data set of the aerodynamic properties needed for input to the final simulation iterations. Other pertinent dynamic rate derivatives were calculated based on theory with some simplifying assumptions. These are listed in Table 2. The refined simulation verified that the vehicle was aerodynamically stable and capable of achieving the flight profile.

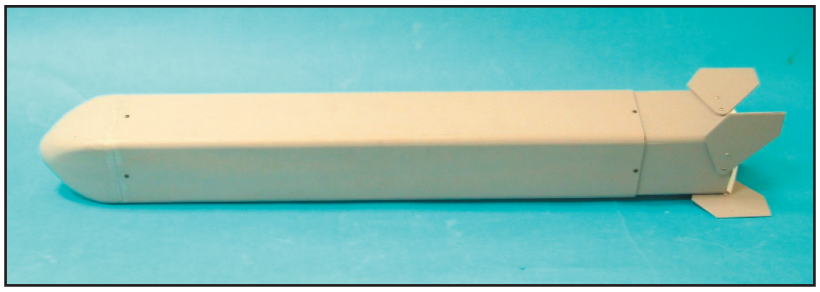

Fig. 8 — VLIIRDT wind tunnel model (half-scale)

Table 2 — Aerodynamic Rate Derivatives

C_{Mq}	–69.41	Pitch damping
C_{Nq}	16.77	Normal force
C_{Lp}	–1.00	Roll damping

4.2.2 Rocket Motor Selection

Once the conceptual changes mentioned in the previous section were made, the simulation was run with the new nozzle configuration and a single rocket motor. The commercially available rocket motor selection was limited, but two models from Aerotech were compared using the simulation. Figure 9 shows the thrust profiles.

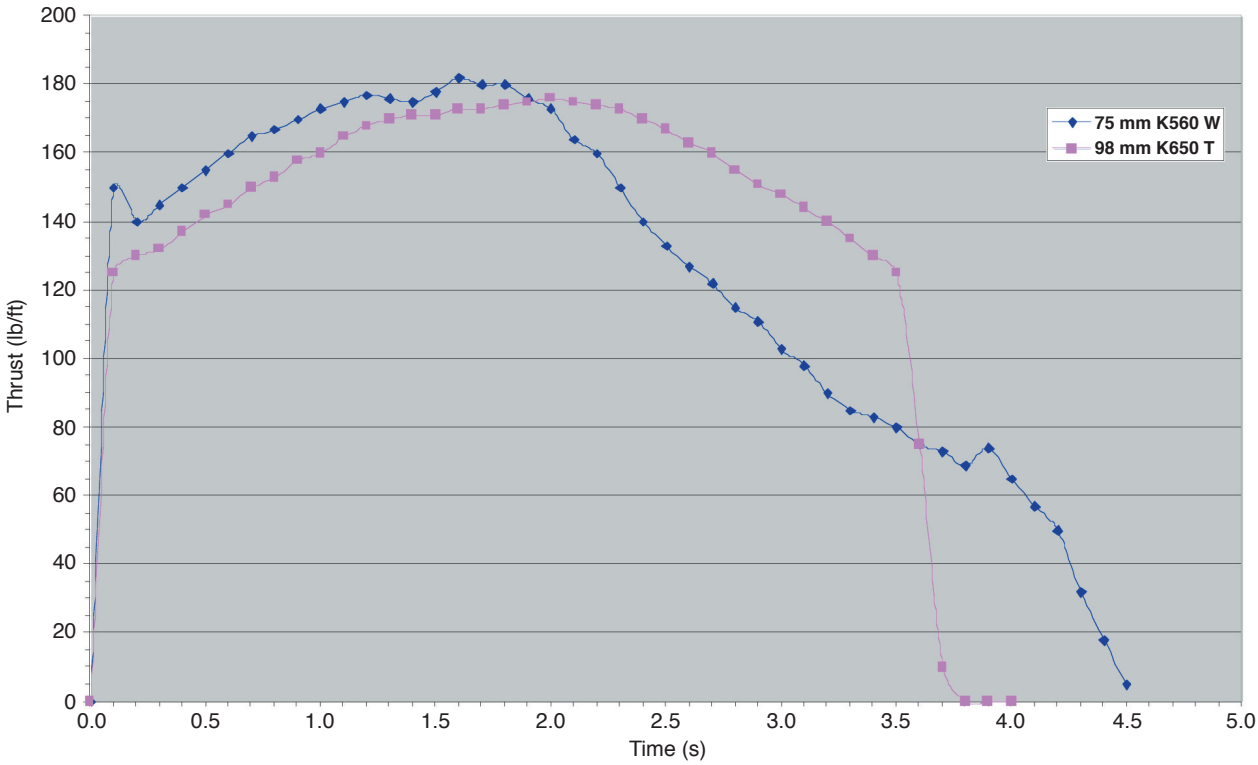

Fig. 9 — Rocket motor thrust profile comparison

The Aerotech K560W motor was chosen for its longer burn time and slightly higher initial thrust. It has the following specifications:

- Diameter: 2.95 in.
- Length: 16 in.
- Weight: 6.12 lb
- Total impulse: 575 lb-sec
- Burn time: 4.5 s

The simulation showed that this motor would complete the mission, achieving the flight profile and a distance of 1,400 ft downrange in approximately 8 s. Once the motor was chosen, its specific weight and thrust curve were used in subsequent simulations. Figure 10 shows the motor.

Fig. 10 — Rocket motor hardware

4.2.3 GFCS Components

The study concluded that 5 lb of thrust per nozzle were adequate for achieving the flight profile. Calculations showed that this thrust could be generated with a nozzle using 800 psi of gas pressure if the exit diameter was at least 0.171 in. A nozzle was designed that had the following parameters:

- Inlet pressure: 800 psi
- Exit diameter: 0.171 in.
- Throat diameter: 0.074 in.
- Nozzle area ratio: 5.37

Bench testing confirmed that the nozzle produced the predicted amount of thrust, and the design was used for the final configuration. The bench test results were also used to refine the simulation.

Once the system's operating pressure was established, the gas tank and regulator for the GFCS were selected. Commercially available integrated combinations of carbon filament-wound tanks and inline regulators are used in the paintball market. An immediately available integrated tank and regulator combination was selected that had the following specifications:

- Maximum tank operating pressure: 4,500 psi
- Tank volume: 88 $in.^3$
- Regulator output pressure range: 200 - 1200 psi
- Empty weight: 3.5 lb

Bench testing showed that this tank and nozzle combination yielded a total impulse of 48.2 lb-sec available at the desired output thrust. This impulse may prove marginal in accomplishing the mission under all environmental conditions with a full payload, but was determined to be well within range for preliminary

testing. Larger compatible tanks are available from the manufacturer (Carleton Technologies – PTD, Inc.) and could be easily replaced within the available space in the vehicle for full-up testing. Figure 11 shows the tank and regulator used in the vehicle.

Fig. 11 — Integrated tank and regulator

4.2.4 Recovery Parachute Sizing

The parachute must slow the vehicle's descent to less than 10 ft/s for minimum damage to the vehicle upon touchdown. Assuming the use of a round canopy, a sizing study was conducted to determine the size of the canopy and its weight. Calculations showed that a 50-lb vehicle could be slowed to 9.5 ft/s with a 22.5-ft diameter canopy. The HX-400 canopy manufactured by Butler Parachute Systems is 22.6 ft in diameter and has a 400 sq. ft surface area. This canopy weighs approximately 6.4 lb and has approximately 3 lb of containment and deployment equipment. The total parachute system weight was approximately 12 lb. The chute packed in its containment system is shown in Fig. 12.

Fig. 12 — Packed recovery parachute

4.2.5 Results

The simulation was updated with the specific characteristics of the components selected for the demonstration vehicle. The components immediately available were purchased, and each component was measured for size and weight. The remaining components of the vehicle were selected or designed around the parachute pack, motor hardware, and GFCS tank and regulator assembly. After each component was incorporated into the design, the simulation was updated with its exact specifications. This provided the limitations for some components yet to be selected in the detailed design phase of the effort.

5. DETAILED DESIGN

With the critical geometry of the vehicle determined and some essential components selected, the detailed design stage began by subdividing the vehicle into three components: the fuselage, the nose subassembly, and the aft subassembly. The fuselage contains the gas tank, parachute, and flight computer. The nose subassembly contains the GFCS. The aft subassembly contains the rocket motor mount and the fin group.

5.1 General Construction and Fasteners

The vehicle was constructed primarily of 0.040-in. gage aluminum 6061-T6 sheet metal that is commonly available at machine shops. Solid metal parts are made of aluminum 2024 with T4 and T351 treatments. The tail fins and nose cone are made of fiberglass composites. Some components in the GFCS were made of 316 stainless steel for welding purposes and to withstand exposure to low temperatures as the compressed gas was released.

As shown in Fig. 13, the majority of the structure is held together by a combination of 4-40 PEM nuts and flat-head Phillips screws. PEM nuts are self-clinching nuts for sheet metal and provide low-profile captive fastening, while the flat-head screws help spread the load across a larger area. This combination gives safe, low weight, and unobtrusive joints along the airframe.

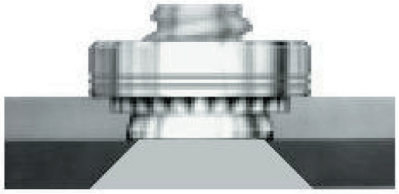

Fig. 13 — Phillips screw and PEM nut-fastening method

The GFCS fasteners are a combination of steel socket-head bolts and washers. This combination is also used in nonsheet metal components and critical load areas, such as parachute attachment points and rocket motor support points. Because some disassembly of the vehicle was expected throughout construction, integration, and testing, permanent fastening methods such as adhesives or rivets were not used.

5.2 Nose Subassembly and GFCS

The nose subassembly consists of the manifold, valves, servo actuators, and nozzles. As many components of the GFCS as possible are housed within the nose cone for compactness, with only the compressed gas tank within the fuselage. The principal specification for component selection is the manifold pressure of 800 psi.

Commercial off-the-shelf hand-operated valves were available that could operate under this pressure. To develop the system quickly at the lowest cost, these valves were adapted for use with R/C servomotors. This would provide effective control of the proportional valves provided that the servos could produce adequate torque to operate the valves. Small stainless steel quarter-turn valves manufactured by Swagelok with the following specifications were selected:

- Operating pressure: 3,000 psi
- Weight: 0.26 lb
- Maximum Cv: 1.4
- Maximum dimension: 2.17 in.

This valve was mated to one of the newest JR digital servos designed for radio-controlled aircraft. The DS8411 Ultra Torque Digital servo, currently the strongest standard-size servo available, has the following specifications:

- Torque: 155 oz/in.
- Speed: 0.18 s/60 deg
- Pulse rate: 250 Hz
- Voltage required: 4.8 V
- Weight: 2.03 oz
- Size: 0.75 in. × 1.54 in. × 1.36 in.

Figure 14 shows the GFCS. The gas from the regulator is fed into a manifold custom designed by Manastrip Corporation. The manifold is made of aluminum and ported to accept the six valve assemblies and the gas supply hose. The servos (shown in black) are connected to an adapting piece that mates the servo's output arm with the valve's handle (shown in green). The valve was fitted with an adapter to mate the valve's tubing port to the manifold's 1/4-in. NPT threads. Six of these servo/valve assemblies are attached directly to the manifold, and each feeds the 800-psi gas to a nozzle using a fitted steel tube bent to the shape of the route from the valve to the nozzle. The steel tube was welded to the inlet of a nozzle for durability and strength. Support brackets were added to support the tubes and mate with the nose bulkhead.

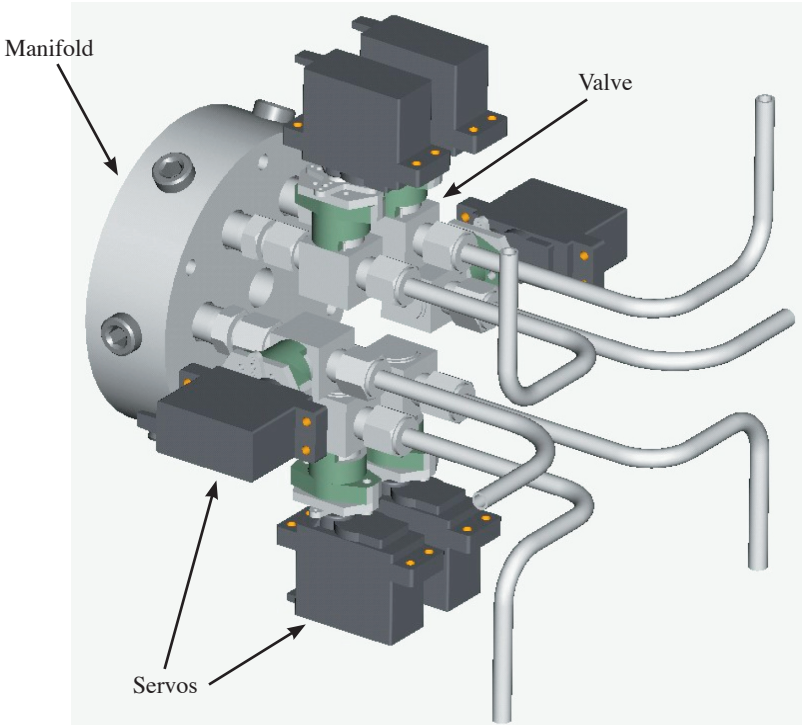

Fig. 14 — GFCS manifold and valve assembly

The nose bulkhead supports the GFCS, holds the nozzles, and joins the nose cone with the fuselage. The bulkhead was designed to contain six nozzles in the configuration shown in Fig. 5. The nose bulkhead also has attachment points for two parachute harness straps.

The six servos consume most of the power used by the vehicle. The current draw of the servos and the anticipated amount of running time, shown in Table 3, determined the required battery capacity. A 5-cell, 2,500-mAh pack provided the power necessary for extended testing and field troubleshooting. Covering the GFCS is a nose fairing made of G-10 fiberglass. The nose cone is attached to the nose bulkhead using flat-head Phillips screws.

Table 3 — Servo Battery Drain

Servo Activity	Current Draw (mA)	Running Time (min)	Battery Drain (mAh)
Moving (3 servos)	4500	5	375
Idle (6 servos)	1800	30	900
		Total	1275

5.3 Fuselage Section

The fuselage must contain all of the components used in the test phase of the vehicle (such as the flight computer, the parachute, and the compressed gas bottle) and be able to withstand the flight loads imposed on it. The largest loads the fuselage will experience are the propulsive forces generated by the rocket motor during flight and the loads from the parachute opening at the end of the flight. Propulsive forces act along the vehicle's longitudinal axis primarily at the junction of the fuselage section and the aft subassembly where the rocket motor is located. Parachute opening loads pull on the top of the vehicle at the nose bulkhead and the aft subassembly, which causes a bending force along the vehicle longitudinal axis.

The main components of the fuselage, shown in Fig. 15, are two U-shaped sheet metal halves that fasten together, giving the fuselage a square cross section. There are four approximately evenly spaced bulkheads installed inside the fuselage to strengthen it and prevent buckling during parachute opening. The two center bulkheads divide the fuselage into three different compartments. The front compartment houses the GFCS tank and the batteries. The middle compartment holds the parachute, and the aft compartment holds the flight computer and IMU. The top cover of the fuselage is divided into two sections: the front section, which acts as a hatch to provide access to the GFCS tank and batteries; and the rear section, which contains an opening through which the parachute is deployed. The parachute opening is covered by a lid that is attached by a hinge at the third bulkhead. It is latched closed by a servo installed at the second bulkhead. The pilot deploys the parachute using the landing gear channel in the radio receiver to actuate the servo. The front hatch runs between the nose subassembly and the first bulkhead on top of the vehicle. Since it involves three layers of sheet metal, this joint's fastening method differs slightly from the rest of the vehicle.

A prominent feature of the fuselage is the large number of fasteners, which are used to join the fuselage halves together, to attach the sheet metal bulkheads to the vehicle, and to mate the aft subassembly with the fuselage. Approximately 380 fasteners were used in the fuselage and aft subassembly and 130 in the nose subassembly. The fasteners add stiffness to the thin walls of the fuselage to help prevent it from buckling.

Mounting hardware for internal components was not designed at this point. This was postponed until later in the integration phase to properly locate the components.

5.4 Aft Subassembly

The aft subassembly, shown in Fig. 16, contains the rocket motor and stabilizing fins and must transmit the corresponding propulsive and aerodynamic loads to the fuselage. The fins are held outside the body and are deployed by rotating outward by springs contained inside the vehicle. The aft subassembly's cross section is smaller than the fuselage to allow the fins to fit flush with the fuselage.

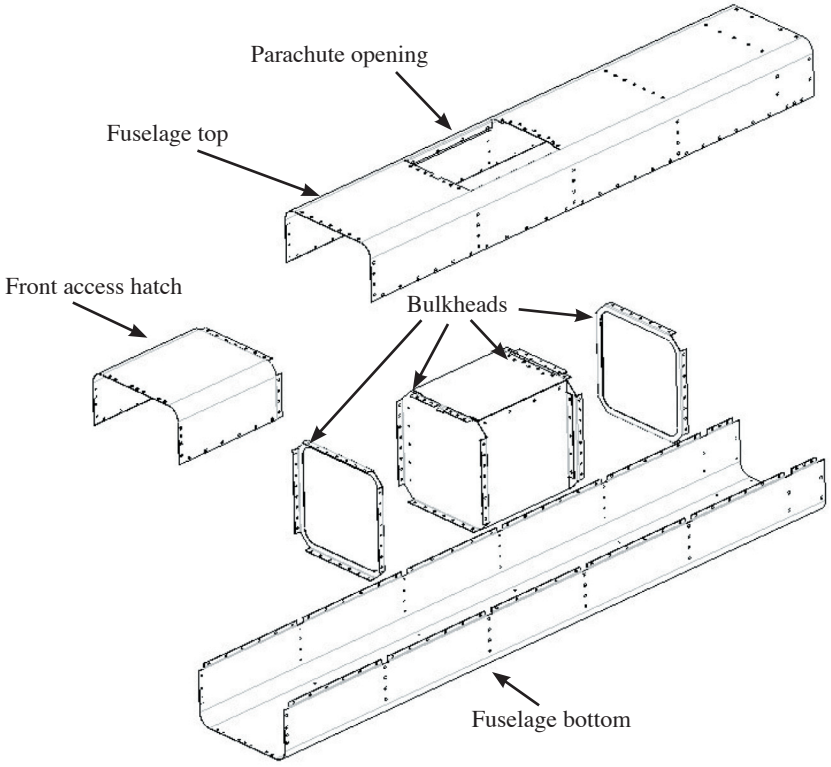

Fig. 15 — Fuselage parts

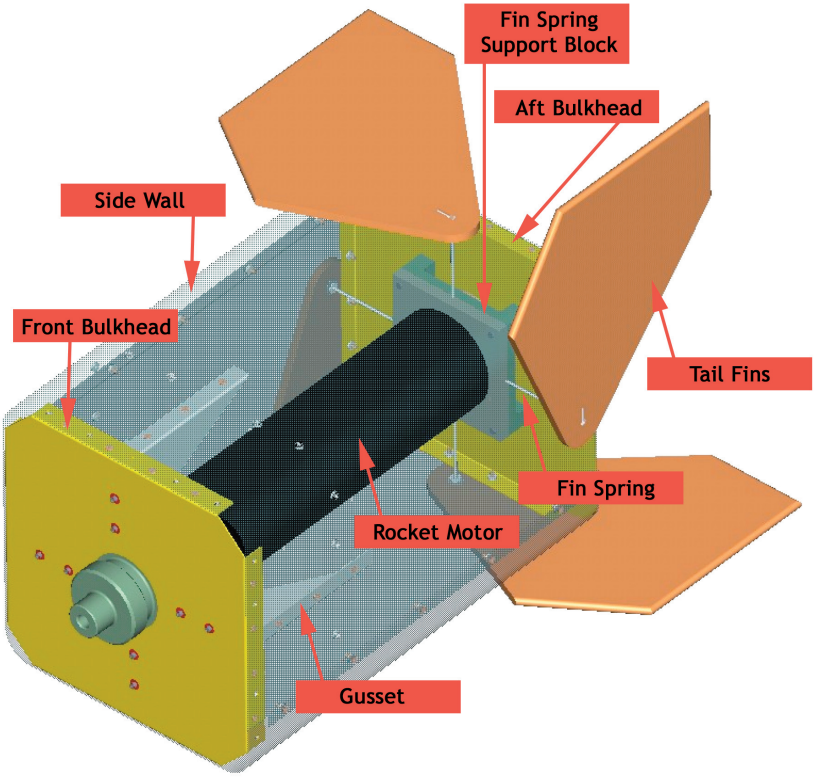

Fig. 16 — Aft subassembly

The aft subassembly consists of two L-shaped sections that fasten together to form the sidewalls. The front bulkhead attaches to the front of the rocket motor and mates with four gussets to provide strength and transmit the loads to the sidewalls. The aft bulkhead attaches to the motor from the rear via a mating ring and transmits loads from the motor to the sidewalls. The ring also mates the motor to the fin spring support block, which provides the pivot axes for the springs. Because the aft section has a smaller cross section to accommodate the fins, eight wooden shim blocks fill the space between the aft subassembly and the main fuselage section.

The rocket motor has a maximum thrust of 180 lb applied at two points in the aft subassembly. It pushes on the front bulkhead, which is fastened to the side walls. Because of the thin construction, this bulkhead had to be stiffened by four gussets that also transmit the loads to the sidewalls through the fasteners. The second point where the loads are transmitted is the fin spring assembly in the rear. Figure 10 shows the rocket motor hardware, which has a gold-toned ring that holds the nozzle of the motor. The ring pushes on the fin support block, which is attached at the aft bulkhead with four bolts. The aft bulkhead is attached to the side walls with 16 screws. The entire subassembly fastens through the eight wooden shims to the fuselage to transmit the tail loads to the rest of the vehicle.

5.5 Flight Computer

The flight computer was the PC-104 stackable, single-board computer, which has the input/output capabilities to read data from all of the sensors and store it internally, as well as transmit it to the ground station via a wireless modem in the event that the data could not be downloaded from the computer after the flight. This is essentially a PC-compatible 5×86 133-MHz system with 32 MB of RAM. The stackable format makes the computer expandable with compatible I/O cards to meet the data handling needs and is commonly used in the unmanned aerial vehicle (UAV) industry for its performance, weight, and size. The input and output sensors listing the quantity and type of connection are shown in Table 4.

Table 4 — Flight Computer Input/Output Requirements

Component	Quantity	Model	Protocol/Connection
IMU	1	Crossbow IMU400CC-200	Serial RS-232
GPS receiver	1	CMC ALLSTAR OEM	Serial RS-232
Pressure sensors	5	Motorola MPX-4115AP/MPX-5010	A/D conversion
Wireless modem	1	FGRO9CS	Serial RS-232
Servo pulsewidths	6	JR DS8411	Timer

A QMM-10 timer card was used for PWM reading/writing of the servos. The data from the pressure sensors were acquired using a MM-16-AT analog-to-digital converter card. An EMM-XT-4 serial port card connected all of the RS-232 devices. All of the components are stacked together with the single-board computer.

Three circuit boards were custom-designed to interface the sensors with the computer. The first board was used to mount all pressure sensors. The second board contains opto-isolators to prevent the computer signals from interfering with the servos. The third board contains two DC-to-DC converters to regulate the 12 VDC and 5 VDC power inputs needed by the different components. Table 5 lists the power requirements of the various components and the maximum output of the DC/DC converters.

Table 5 — Flight Computer Power Requirements

Component	Quantity	Volts	Amps	Watts
Computer	1	5	1.200	6.000
Timer card	1	5	0.290	1.450
Serial card	1	5	0.080	0.400
A/D card	1	5	0.320	1.600
GPS card and antenna	1	5	0.240	1.200
IMU	1	12	0.167	1.999
Wireless modem and antenna	1	12	0.650	7.800
Baro sensors	5	5	0.005	0.025
			TOTAL	20.474
DC-DC Converters		Volts Out	Amps Out	Watts Out
Datel UMP-5/6-Q48	1	5	6.000	30.000
Power trends PT3105	2	12	1.200	28.800
Supply required		24	1.024	20.474

The DC power for the computer and the sensors was provided by a 20-cell pack of 1,000-mAh batteries that powered the system for approximately one hour with a 20 percent safety margin on current draw. This duration was chosen to accommodate ground testing procedures and troubleshooting. The power requirements are listed in Table 5.

6. MANUFACTURING, ASSEMBLY, AND INTEGRATION

Once the detailed design for the vehicle was complete, production drawings were completed. The nose subassembly drawings were released first, since the GFCS would have to be function-tested extensively after the parts were received and assembled. Fit checks were performed on all of the components as they arrived.

6.1 GFCS Manufacturing and Assembly

With its predominantly solid metal design and many commercial parts, GFCS manufacturing and assembly was straightforward. Figure 17 shows the nose subassembly without the fiberglass nose cone fairing. The total assembly weighed 11 lb.

6.1.1 GFCS Performance Testing

After the GFCS system was assembled, it was tested in a force balance. The following are the results of the measurements:

- Maximum nozzle thrust: 6.2 lb
- Maximum flow rate: 0.09 lb-sec
- Response: 1.8 Hz
- Specific impulse: 59 s

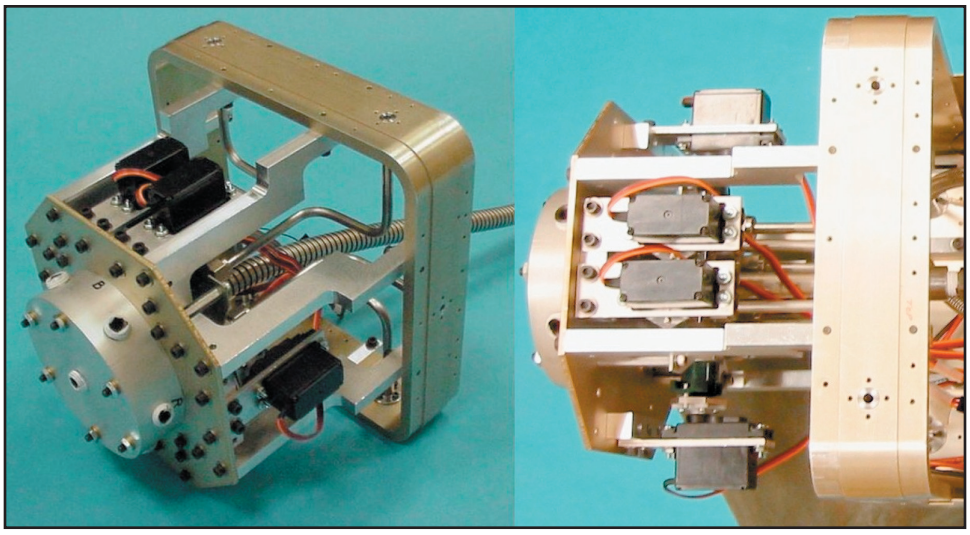

Fig. 17 — Nose subassembly

The thrust measured exceeded the design goal of 5 lb, most likely because of a higher manifold pressure than the regulator indicated. Because the thrust was higher than anticipated, the resulting flow rate was not sufficient to generate the maximum thrust with more than two fully opened valves. However, based on the VLIIRDT computer simulation, the thrust was sufficient to control the vehicle in the initial field tests.

The actual input/output response of the GFCS was less than the original 5-Hz requirement. This was due to the actuator. It was determined that this slower performance was acceptable for initial testing, given the advantages of the easy interface to R/C, small form factor, and light weight. Even with the best R/C servos available, the torque provided is insufficient to overcome the valve friction when the system is fully pressurized. A possible solution is the use of more powerful actuators, such as geared stepper motors with higher torque output, at the expense of more weight, and greater mechanical and electrical complexity. Another option is using lower performance valves that will have less friction and allow some acceptable amount leakage that can be compensated by a larger-volume compressed gas tank. These solutions could be incorporated into the vehicle design after the experimental stage.

6.2 Airframe Manufacturing and Assembly

All airframe parts were first painted, and the PEM nuts were installed along the inner flanges at places where two pieces of sheet metal were joined. The aft subassembly fuselage sections were joined to check the fit with the fuselage section. After all of the bulkheads were installed, the shape of the vehicle was measured to verify that it was consistent with the design.

The second and third bulkheads were installed to form the parachute compartment. A lid was attached to the third bulkhead with a hinge. A fit check with the parachute pack revealed that the fit was too tight and would not allow the pack to be pulled out of the compartment by merely exposing the pilot chute to the air stream. The compartment was enlarged in length by 5/8 in. and in width by 1/2 in. to alleviate this restriction. The parachute latching servo was then mounted to the second bulkhead with plastic brackets.

6.2.1 Aft Subassembly

The aft section was assembled by mating the two L-shaped walls together and then installing the tail fins. In the original design, a set of torsion springs was used to rotate the fins outward from the body into the

wind stream. Function testing of the assembled section showed that the torsion springs deformed when the fins were in the stowed position, preventing them from rotating outward. The torsion springs were replaced with coiled springs—one end of the spring was held in place by the support block attached to the rear of the rocket motor inside the fuselage, and the other end protruded through the skin and into the fin. A slot in the fuselage allowed the spring to rotate the tail fin properly. Figure 18 shows the tail fins.

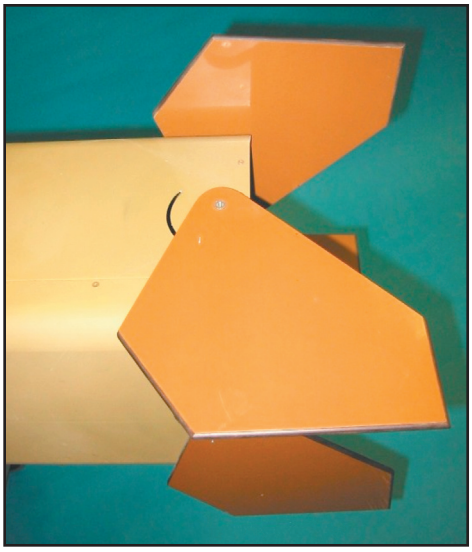

Fig. 18 — Fin group

6.3 Flight Computer Packaging and Assembly

The flight computer components were assembled in two stacks (one for PC-104 components and one for custom boards) and packaged with the GPS receiver and modem into a compact chassis. The chassis was open to allow connections to the computer from the components located in different parts of the vehicle. The GPS receiver and wireless modem were connected directly to the serial card in one of the stacks. The only component that resides outside of the chassis is the IMU. The assembled computer in the chassis weighed 3.35 lb.

6.4 Vehicle Integration

The flight computer and the GFCS were mounted in the vehicle for bench testing. The two systems are linked together by a cable that transmits the servo signals to the timer card for recording the flight data.

6.4.1 Flight Computer Integration

The flight computer was mounted in the fuselage section between the aft subassembly and the parachute compartment, through the fourth bulkhead. It was installed by attaching rubber vibration mounts (Fig. 19) to four points on the computer chassis and fastening them to the bottom skin. The IMU was fastened with brackets to the third bulkhead just behind the parachute compartment.

The following connections were made:

- Serial + power cable from computer to IMU
- GPS antenna to receiver card
- Wireless modem antenna to modem card

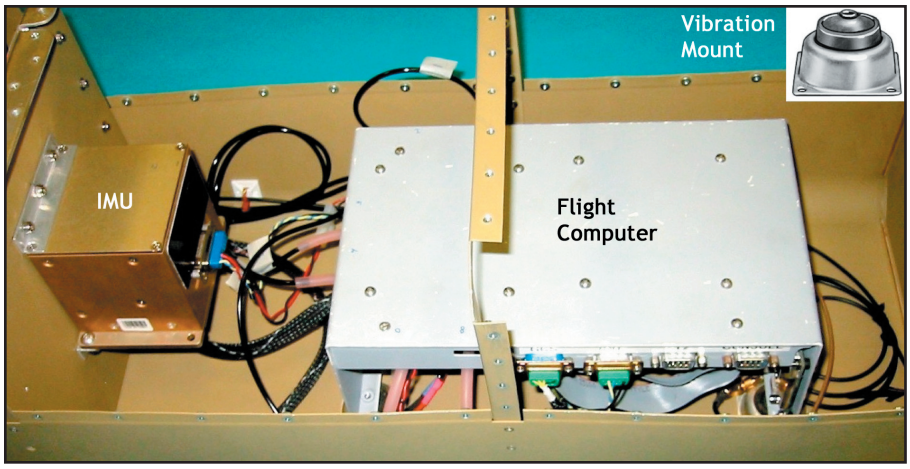

Fig. 19 — Flight computer and IMU installation

- Battery pack to computer power supply card
- Servo pulse width line from GFCS to timer card
- Plastic tubing from pressure taps near the nose to pressure transducer card

The GPS antenna, modem antenna, and computer power supply switch were installed on the nose cone of the vehicle for unobstructed access when the vehicle was sitting vertically in the launcher. A Pitot probe was installed at the tip of the nose to measure the free stream air pressure. Four other pressure ports were located in the fuselage between the nose bulkhead and the first fuselage bulkhead. The servo pulse-width sensing line, consisting of six lines shielded and bundled together, was connected to the opto-isolator board and to the GFCS R/C receiver and the servos using a Y-harness. For balance purposes, the flight computer batteries were placed in the front compartment between the GFCS and the first fuselage bulkhead. A switch harness connected the power supply to the computer's power supply board.

The electrical harnesses and the pressure ports' plastic tubing were passed through the nose bulkhead into the space between the fuselage bulkheads and the lower skin and into the aft compartment where they were connected to the computer.

6.4.2 GFCS Integration

The nose subassembly was mounted by fastening the nose bulkhead to the bottom fuselage half. The top half of the bulkhead would be fastened when the front hatch was installed. The tank was mounted using a set of bulkhead plates to secure the neck of the tank aft of the regulator at the first bulkhead and to support the round end of the tank. The supply hose was connected between the gas tank regulator and the GFCS manifold. Figure 20 shows the assembled hardware.

The Y-harness mentioned in Section 6.4.1 receives the R/C servo signals from the receiver and sends them to both the servos and the opto-isolator board, where they are read by the timer card and stored by the computer. The battery pack for the servos was mounted in the same front compartment to help balance the vehicle. The switch for the R/C system was installed in the nose cone for easy access.

6.5 Additional Subsystems

The parachute was installed by using a karabiner to attach the two front straps' flanges inside the nose bulkhead and by securing the two rear straps to small mounting points inside the aft subassembly. After the

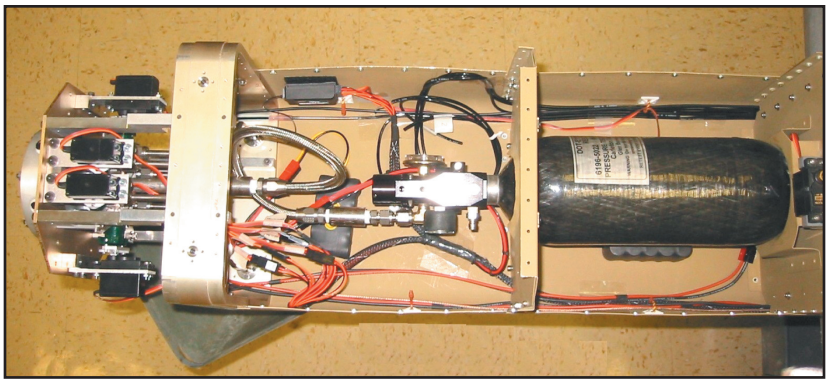

Fig. 20 — GFCS installed

parachute was installed, the top of the fuselage was attached. The parachute lid was closed, and the parachute straps were taped to the top half of the fuselage around the free edge of the lid. Figure 21 shows the complete vehicle before the top of the fuselage was attached.

A launcher was designed and fabricated at the Naval Research Laboratory (NRL) to provide the stabilization needed in the first seconds of the vertical launch. The launcher consisted of two U-shaped sheet metal sections, made of 1/8-in. thick aluminum 6061-T6, fastened together to form a tube. There are cross members at the bottom of the launcher to support the vehicle from below and allow the exhaust gases to escape. The launcher is secured to the ground with stakes that are driven through the four supports. Figure 22 shows the launcher.

7. VEHICLE TESTING

After the subsystems were successfully integrated into the vehicle body, bench testing of the vehicle was conducted. After bench testing was completed, a series of flight tests were conducted. The goal of flight testing was confirmation that the vehicle was stable in flight and could be controlled using the GFCS.

7.1 Preflight Testing

Bench testing began by powering up the flight computer, GFCS, and ground-station computer. A modem link was established to confirm that the telemetry system was transmitting properly for in-flight recording of vehicle sensor data. The ground station software confirmed the wireless modem link and proper sensor functioning by displaying the data collected from the sensors. Then the GFCS servos were actuated to ensure

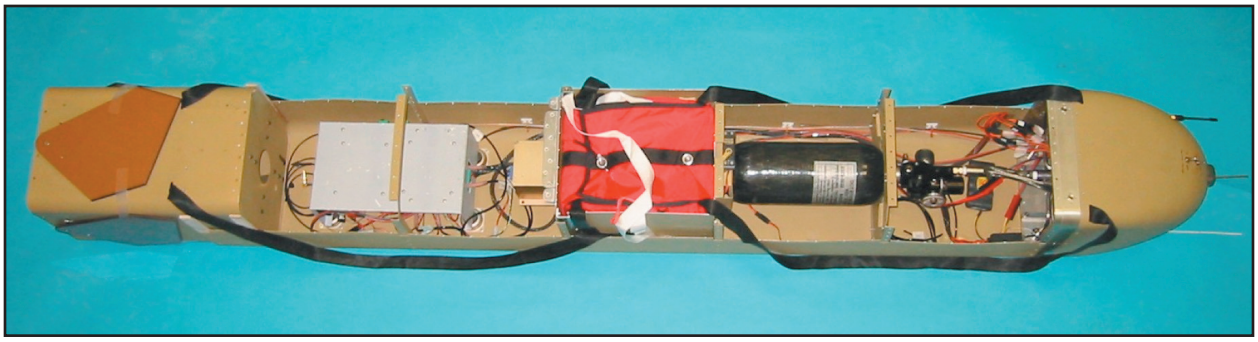

Fig. 21 — Integrated VLIIRDT test vehicle

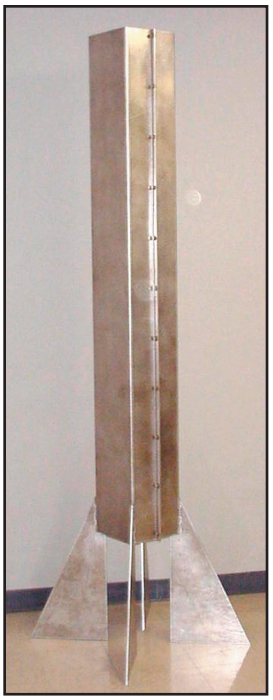

Fig. 22 — VLIIRDT launcher

that the system recorded the servo pulse widths. Figure 23 shows the ground station readout of the sensor data.

A series of range checks that repeated the bench testing sequence at increasing ranges were conducted to ensure that there was a reliable control link from the R/C transmitter to the receiver on the vehicle. During these tests, an oscillation of approximately 15 percent full-scale span at 2 Hz was present in all GFCS servos when both the wireless modem and the R/C system radio links were established. The servos responded to commands sent via the R/C system, but when the servos were idle, the oscillation continued. After numerous attempts to electromagnetically shield the R/C system components, the modem antenna was separated from the R/C system by moving it from the nose to the aft of the vehicle. With the modem antenna mounted in the aft-most bulkhead of the aft subassembly, the oscillations were eliminated.

When conducting further tests to verify control range, it was found that the R/C range was dramatically reduced when the flight computer was powered. It was thought that radiation from the computer could be the cause of the interference. The computer chassis was better grounded and covered with Eccosorb® shielding to reduce its electromagnetic radiation output; this improved the range. The interference effects were eliminated entirely by moving the R/C antenna approximately 30 in. from the vehicle. An extension rod was mounted to the vehicle, and the antenna was mounted on it. A full-range check was successful, and the vehicle was ready for flight testing.

7.2 Flight Testing

The flight tests were conducted at Army Research Laboratory's Blossom Point Field Test Facility. Four flight tests were conducted between June 28, 2002 and August 5, 2003.

7.2.1 First Flight

The first flight test was conducted on August 21, 2002. The vehicle was to exit the launcher and fly at a 45-deg angle until motor burnout, at which time the parachute was to be deployed. Because this was the

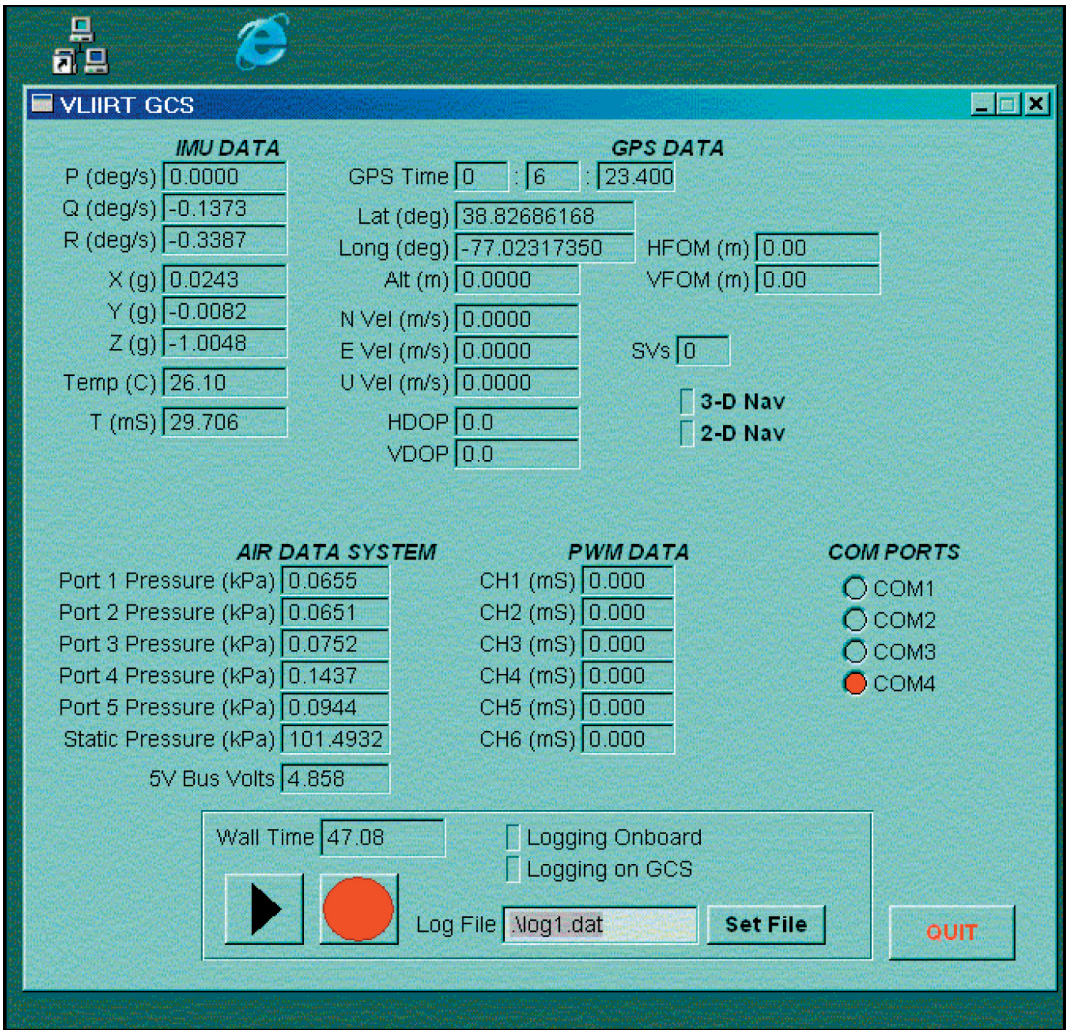

Fig. 23 — Ground control station data display

first flight, the R/C system was set to deploy the parachute automatically if R/C control signal was lost. Immediately after the vehicle cleared the launch tube, the parachute latch opened and the parachute deployed. The R/C signal was lost at some point between the activation of the R/C system after the vehicle was inserted into the launcher and when the motor was ignited. Figure 24 shows the sequence of events.

The pilot chute opening is circled in the top left frame. The top right frame shows the canopy being pulled out of the parachute compartment during the vehicle's climb. When the canopy inflated, it acted as a large air brake that arrested the climb and swung the vehicle around to a short descent and moderate impact with the ground. No useful flight data was gathered during this flight. However, the effectiveness of the parachute system was proven conclusively, since it landed the vehicle with minimal damage in spite of the malfunction.

The vehicle was recovered with some minor structural damage to the first bulkhead and GFCS tank support structure. The tank was replaced because the regulator valve broke and there was a moderate scratch on the epoxy coating, which may have compromised the tank's pressure holding capacity.

7.2.2 Second Flight

The second flight test was conducted on September 25, 2002, after repairing the minor damage from the first flight and troubleshooting the radio interference problems previously described. During preflight system testing prior to launch, the GPS receiver was not functioning. After unsuccessful troubleshooting, the flight test was conducted to prove vehicle control and to obtain the flight data from the IMU.

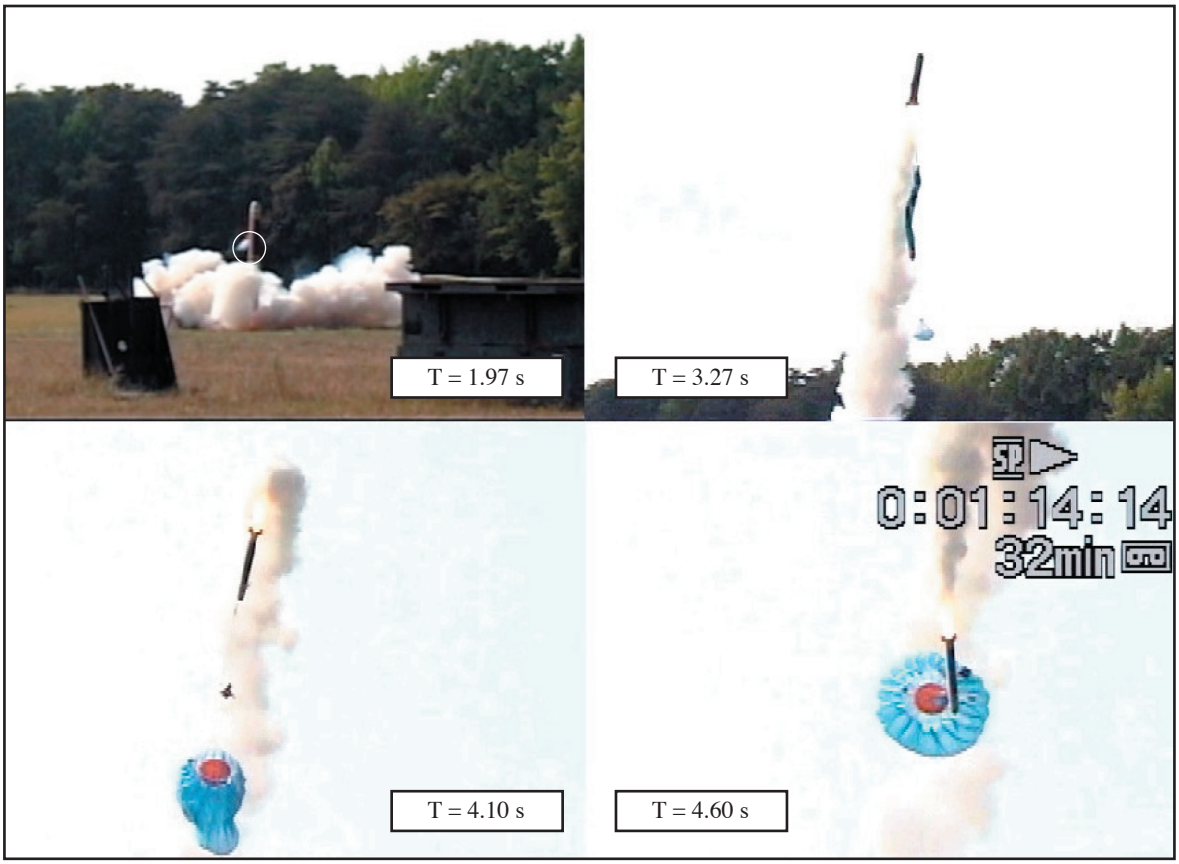

Fig. 24 — August 21, 2002 flight test

Figure 25 shows a sequence of pictures of the flight. After the motor ignited, the vehicle exited the launch tube and immediately began to roll. The pilot successfully reduced the roll rate and gave a pitch-down command to achieve the 45-deg flight. Another pitch-down command was given to deploy the parachute.

The flight lasted approximately 7 s. During most of that period, the pilot was issuing commands to reduce the roll rate. The top right frame of Fig. 25 shows the effect of the second pitch-down command, which resulted in a pitch up because the vehicle was inverted. The parachute deployed properly, and the vehicle was successfully recovered with no damage.

The flight data that were recorded during flight (Figs. 26 through 28) show details of the flight. The three charts show the accelerations, rotation rates, and servo commands, respectively. The event markers on the charts show the different events that occurred during the flight. The important events are the instances where control of the vehicle from the GFCS is shown, such as the roll rate reduction and the pitch maneuver. The two right roll commands shown initiated at 3.75 and 5 s into the flight reduced the vehicle's roll rate along the body axis (the blue "p" line in the angular rate chart), which was so high that it initially saturated the sensor. The effects of the pitch commands are also seen just after 6 s in the accelerations (red az(g) line) and the angular rates (magenta "q" line) charts. Additional flight data showing altitude and accelerations are provided in Appendix A.

This flight test met the goal of proving positive control of the vehicle in powered flight using the GFCS. The high roll rate did not allow enough maneuvering time to pitch the vehicle over at the beginning of the flight, but the response of the vehicle to pitch commands was briefly demonstrated. The reusability of the test vehicle using the parachute was proven conclusively. The vehicle was recovered without any damage after the second flight.

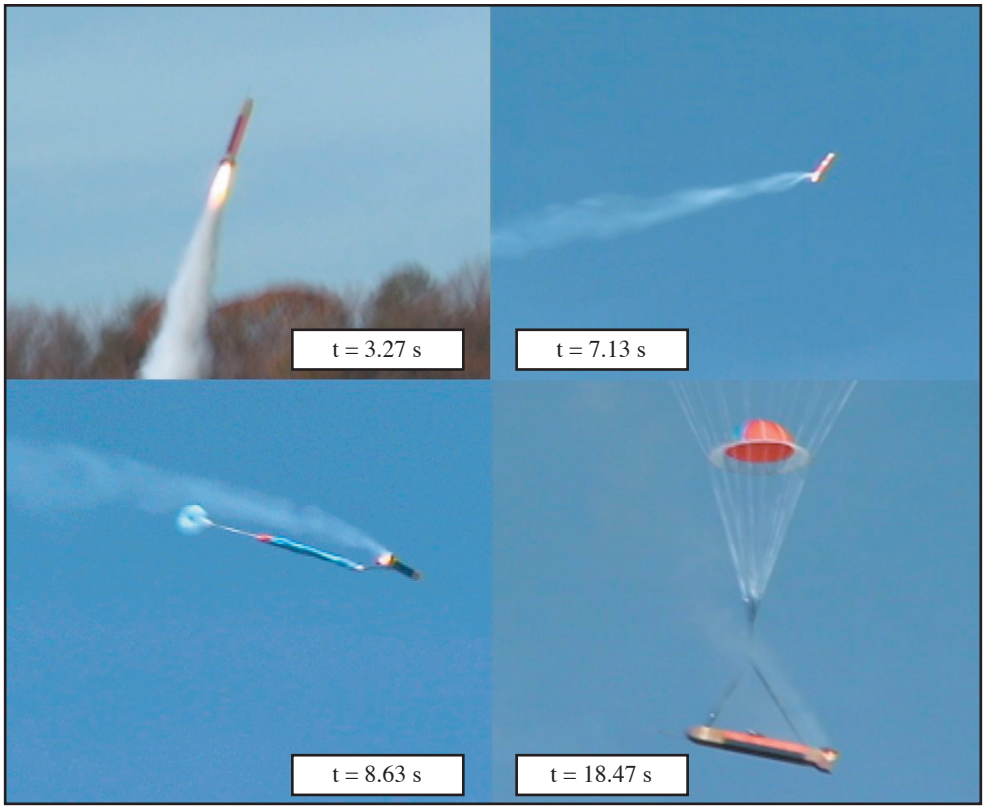

Fig. 25 — September 25, 2002 flight test

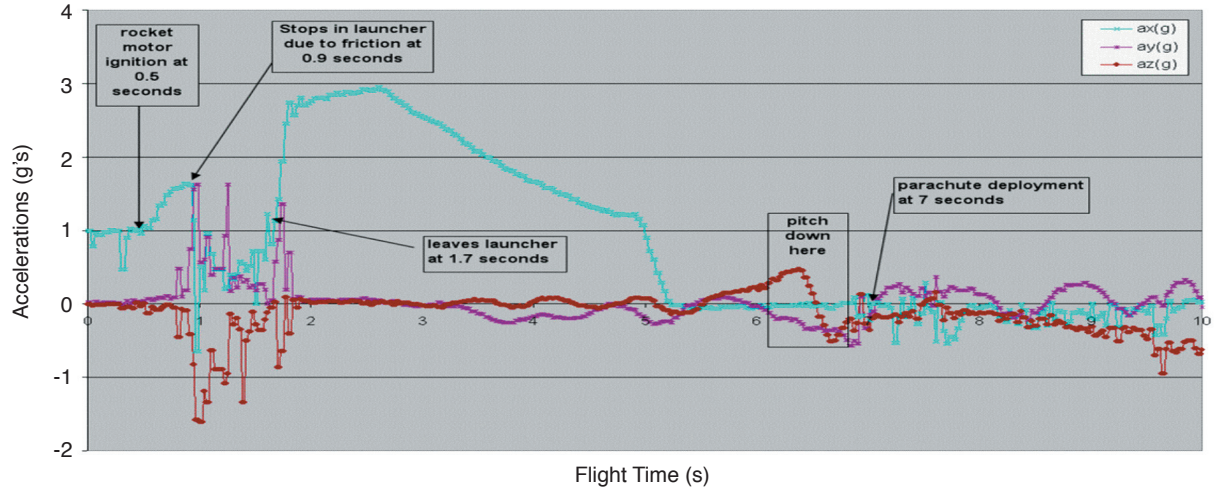

Fig. 26 — VLIIRDT accelerations during flight

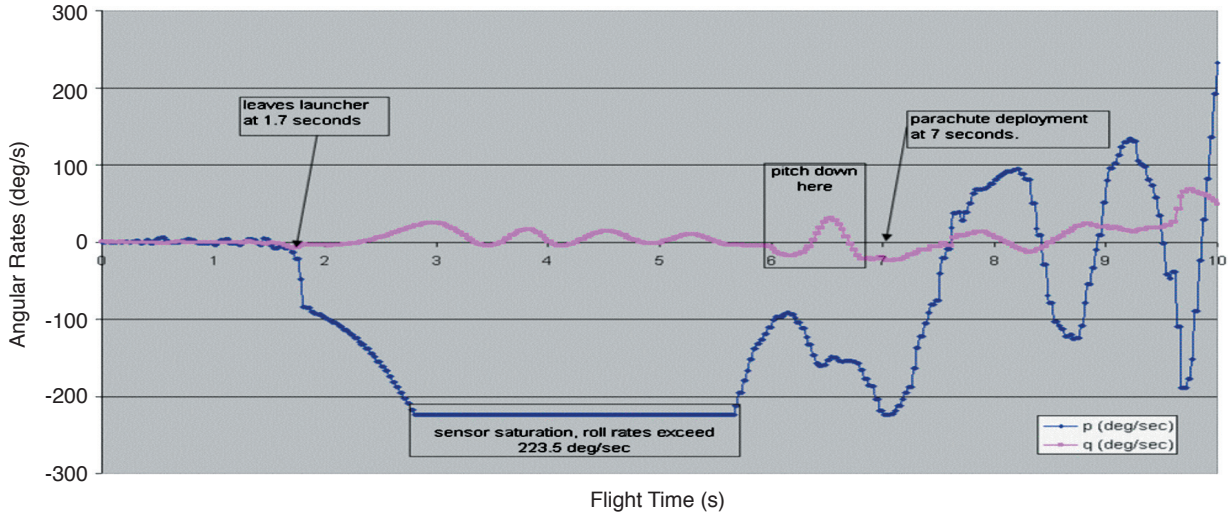

Fig. 27 — VLIIRDT angular rates

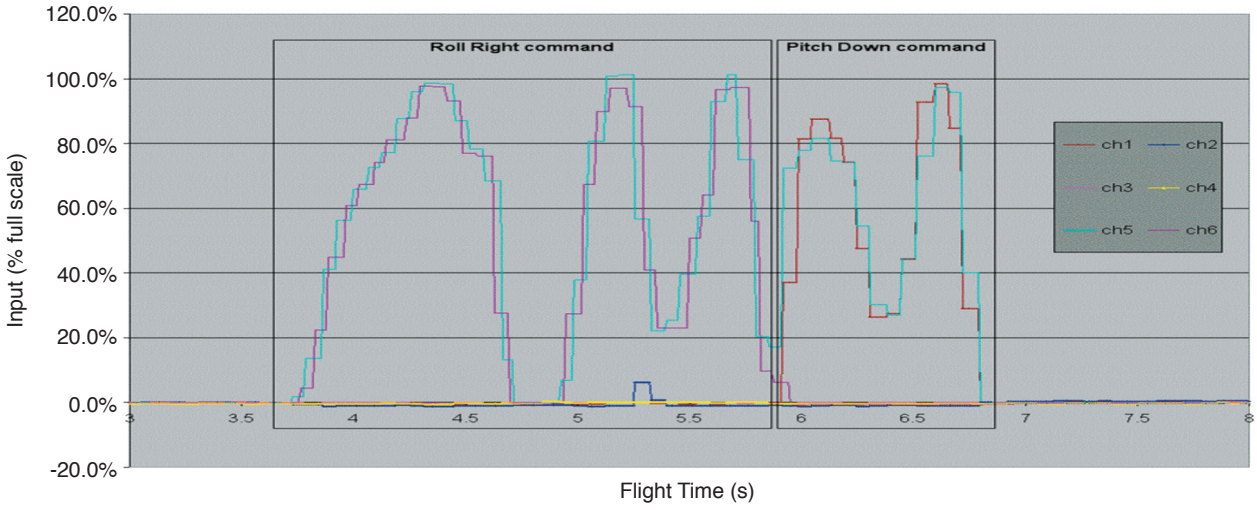

Fig. 28 — VLIIRDT servo inputs

7.2.3 Third Flight

A third flight test was conducted on May 1, 2003, to execute a flight profile that approximates the mission, namely flying parallel to the ground after a 90-deg pitchover. The GPS receiver was tested successfully at the bench prior to the test, but again failed to acquire any satellites at the test range. A similar anomaly (few satellites acquired, then lost randomly) has been seen sporadically on other tests held at Blossom Point. The data provided by the GPS were available from other sensors in the vehicle. Therefore, testing was continued, and the vehicle was launched without the GPS functioning.

In order to minimize the high roll rates observed in the previous flight, slots were made at the corners of the launcher. This allowed the fins to deploy completely before the vehicle cleared the launcher and minimized any roll induced by the fins springing outward from the vehicle body. The high roll rates were still present after launch, however, and the pilot had to take corrective measures during the vehicle's climb. The data charts in Appendix B show the altitude, airspeed, and acceleration data for this flight. Most of the pilot commands were again directed towards reducing the roll, and there was less flight time left for pitch maneuvering. One strong pitch command was issued shortly after motor burnout and before apogee; the resulting change in flight direction is shown in the bottom left image of Fig. 29. After apogee, the vehicle was allowed to gather some speed in a nose-down attitude for better parachute deployment. The parachute was deployed 3 s after apogee and the vehicle descended.

Due to a cross wind that affected both the flight of the vehicle and its descent, the vehicle descended into the trees next to the test range and stopped approximately 30 ft from the ground. The vehicle suffered minor cosmetic damage during recovery.

Fig. 29 — May 1, 2003 flight test

The vehicle was repaired from its recovery damage, and the data was retrieved. The GPS receiver was checked at the bench, and further diagnosis showed that the connection between the antenna and the receiver was not secure and is suspected in the failure to acquire any satellites at the field.

The controllability of the vehicle with the GFCS was demonstrated during the flight to a limited extent. The short duration of the flight and the high roll rate prevented a full evaluation of the GFCS's functionality during a fully simulated mission. The combination of the pilot's reaction time and the high roll rate kept the vehicle from flying the planned trajectory, but the ability of the GFCS to control the vehicle and to make the necessary maneuver was shown.

7.2.4 Fourth Flight

The fourth and final flight of the vehicle was conducted on August 5, 2003, with the goal of achieving the 90-deg pitchover and the horizontal flight downrange. In order to achieve a nearly horizontal flight, the pilot was to issue the pitch-down command immediately after the vehicle exited the launcher before the vehicle could roll. This would approximate a fully functioning autopilot's command sequence.

The corner slots mentioned in Section 7.2.3 were lengthened further to allow the fins to deploy earlier in the tube so that some of the rolling moment could be arrested while still in the tube. The rocket motor was modified by removing the smoke charge, which normally produced black smoke to allow better tracking of the vehicle in flight for video documentation purposes. Otherwise, the vehicle's configuration was identical to previous flights.

Starting at the top left in Fig. 30 and continuing clockwise, the pictures show the liftoff, midway through the pitchover maneuver, the horizontal flight, and the descent from video footage taken from the ground. The vehicle exited the launcher and was immediately pitched down by the pilot to a near-horizontal flight path. The resulting trajectory is shown at the bottom left frame of Fig. 30. This trajectory confirms that the vehicle will be able to perform the intended mission.

The maximum altitude was approximately 120 ft. The parachute was deployed approximately 4.6 s after liftoff at an altitude between 35 to 40 ft above ground level. The parachute slowed the vehicle down and allowed it to impact the ground with only minor damage at approximately 700 ft downrange from the launch position. The flight showed the vehicle's capability to execute a sharp turn and transition to horizontal flight. This flight demonstrated that the vehicle could effectively achieve horizontal flight after a vertical launch using the GFCS.

8. CONCLUSIONS

This effort successfully demonstrated the feasibility of using a gas flight control steering system on a low-cost vehicle that can be launched vertically and then flown horizontally. This permits the vehicle to position decoy materials to counter a threat approaching from any direction. The flight tests demonstrated positive vehicle control by a pilot using an R/C link. Certainly, a low cost autopilot could easily replicate the human pilot's commands. The steering system of a gas reservoir feeding six ports on the nose of the vehicle used only six moving parts to fully control the vehicle's flight. The inherent simplicity of the system resulted in a very robust and reliable vehicle that can be used for development of a decoy system compatible with the next generation of naval ships.

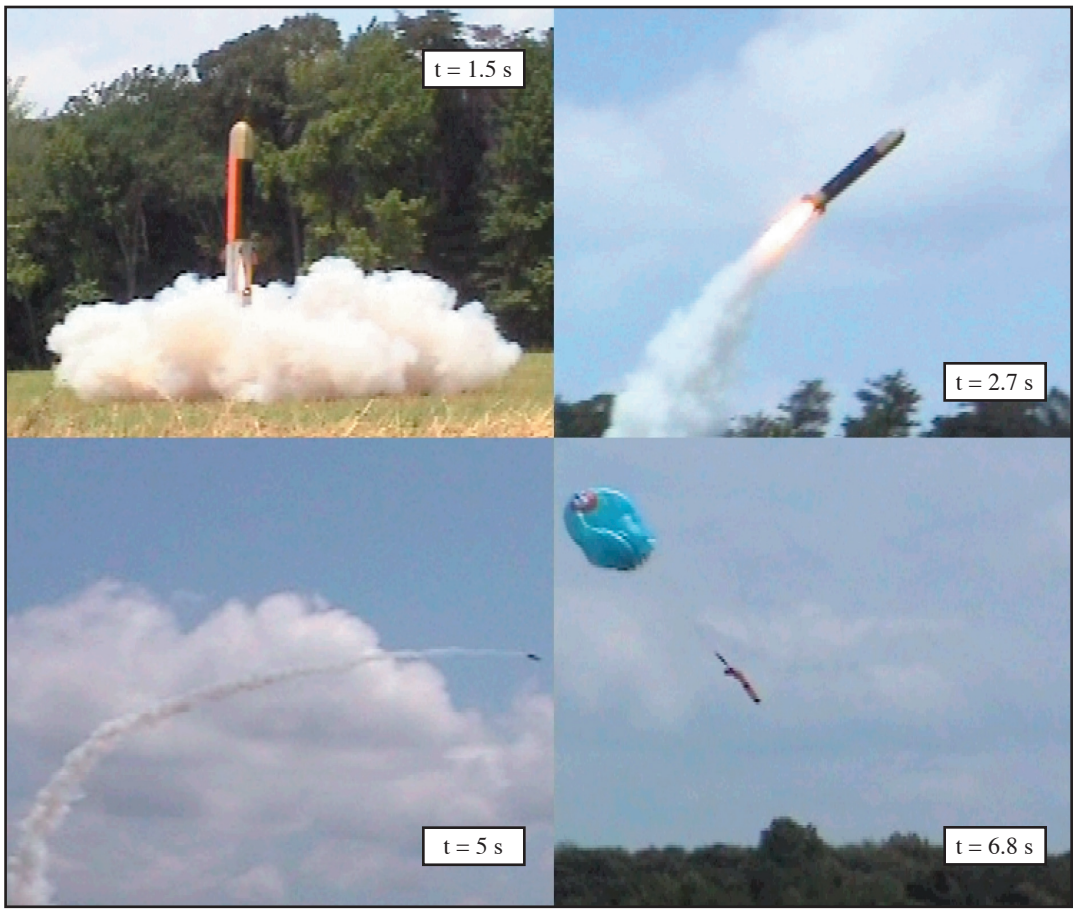

Fig. 30 — August 5, 2003 flight test

9. RECOMMENDATIONS

Due to time and budget constraints, the vehicle was controlled by a pilot in the field tests. Positive control of the vehicle was demonstrated. The implementation of an autopilot would permit the vehicle to achieve all-aspect flight capability and should be the next step of development. The testing of the vehicle yielded many of the parameters necessary for the development of an autopilot (or modification of existing UAV autopilot systems available to NRL).

The design and integration of a payload dispenser into the vehicle would result in a fully functional decoy. Since the vehicle is controlled by using compressed gas, a reservoir large enough to supply the steering system and dispense decoy material is a logical method to investigate. The reservoir needed to hold the extra volume of gas would require a small additional amount of vehicle internal volume and modified hardware to deliver the extra gas. Using gas to dispense particulates is also a very efficient method of dissemination.

The focus for this effort was rapid development and low-cost demonstration. The entire vehicle structure and subsystem components can be improved. The GFCS would require more powerful actuators to provide the necessary response. If mass production were desired, it would be advantageous to have a custom-designed integrated manifold/valve/nozzle/tank assembly that would contain the entire GFCS in a more compact unit.

The stabilizing fins should also be redesigned. A different fin configuration and deployment system would avoid the high roll rate produced by the aerodynamic forces during flight. One configuration would be to have the fins contained internally and deployed linearly outward from the vehicle. This would also improve structural integrity by allowing the airframe to be fabricated as one section instead of a main fuselage and an aft subassembly. Alternatively, larger fins located further forward could increase the roll damping without affecting the pitch stability.

The airframe's sheet metal construction was convenient for this effort, but it required many fasteners; and the alignment of the parts was critical, which made closing the vehicle a time-consuming task. In the field, it would be desirable to have immediate access to the flight computer. A better "button up" system with access to components would be advantageous for field testing and diagnostics. With the constant cross-section fuselage described in the previous paragraph, a composite construction would provide structural integrity while greatly reducing the need for many fasteners and decreasing airframe weight.

The flights showed a reasonable degree of maneuverability with the GFCS in the primary control directions of pitch and roll. Further testing would benefit greatly from computer stabilization and control. Further development of a fully autonomous vehicle with material dispensing capability would be the next step given the proof-of-concept success demonstrated with the current vehicle.

BIBLIOGRAPHY

Aerotech Inc., http://www.aerotech-rocketry.com/customersite/resource_library/Catalogs_Flyers_Data_Sheets/AeroTechCatalog2001a.pdf

Butler Parachute Systems, Inc., http://www.butlerparachutes.com/publicat.htm

CMC Electronics Inc., http://www.cmcelectronics.ca/products-services/custom-elect/allstar-GPS.html

Crossbow Technology, Inc., http://www.xbow.com/Products/Product_pdf_files/Inertial_pdf/IMU400CC.pdf

DATEL, Inc., http://www.datel.com/data/power/ump25-40w.pdf

Diamond Systems Corporation, http://www.diamondsystems.com/products

FreeWave Technologies, Inc., http://www.freewave.com/fgr900oem.html

Horizon Hobby, Inc., http://horizon.hobbyshopnow.com/products/description.asp?prod=JRPS8411&ptab=tech#tabs

Motorola, Inc., http://e-www.motorola.com/webapp/sps/site/taxonomy.jsp?nodeId=01126990368716

Texas Instruments Inc., http://focus.ti.com/docs/prod/productfolder.jhtml?genericPartNumber=PT3105

Appendix A

SEPTEMBER 25, 2002 FLIGHT TEST DATA PLOTS

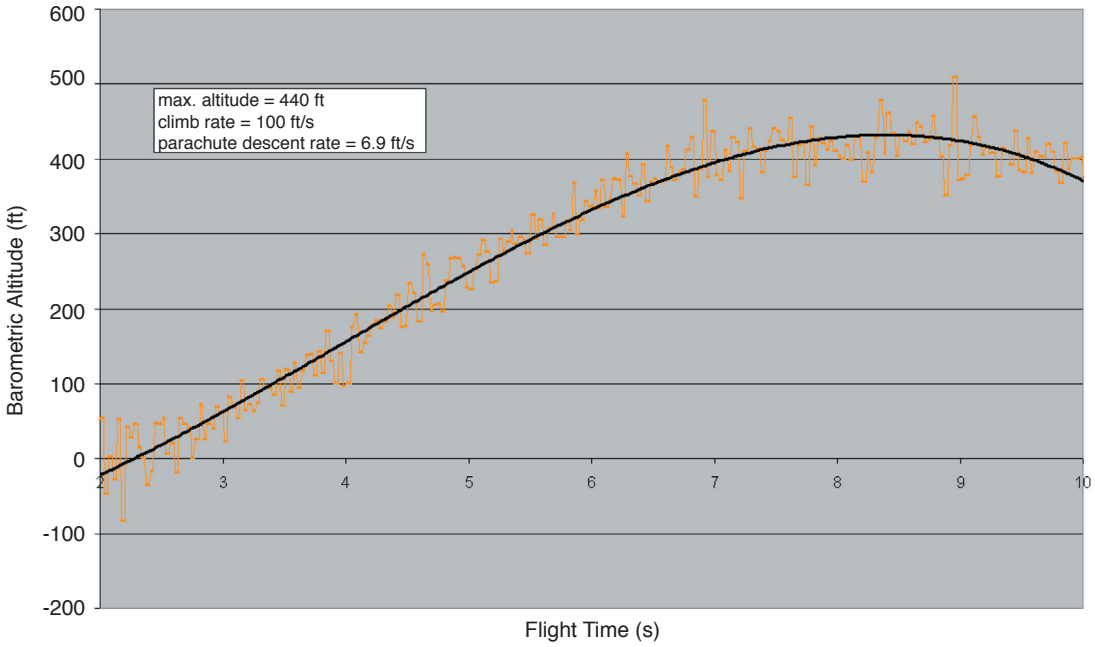

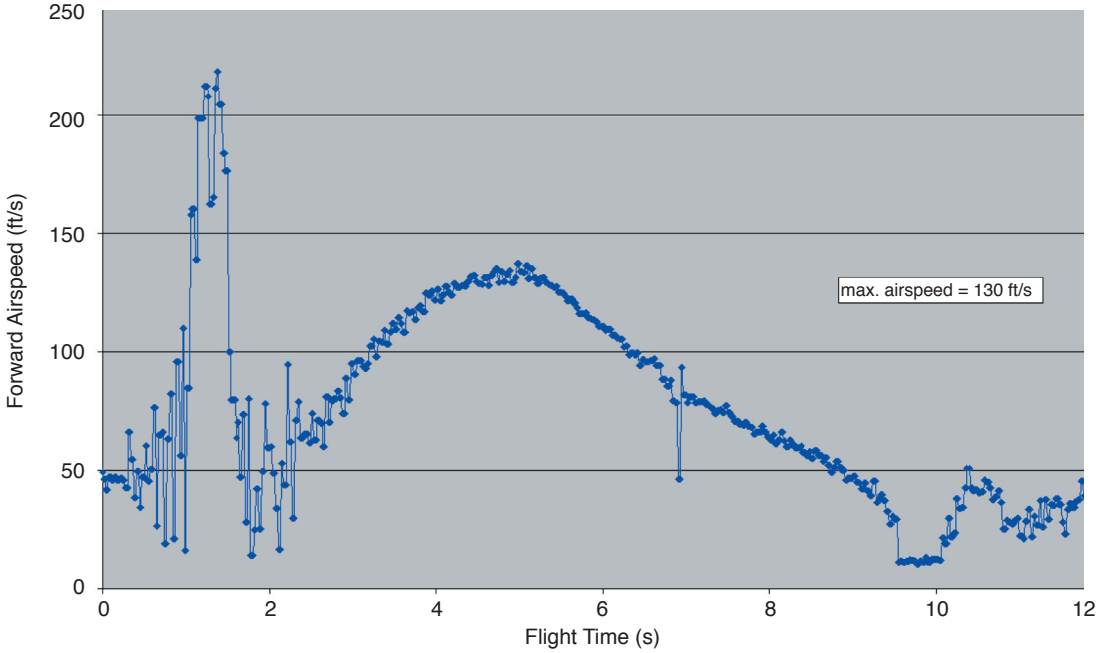

Appendix B

MAY 1, 2003 FLIGHT TEST DATA PLOTS

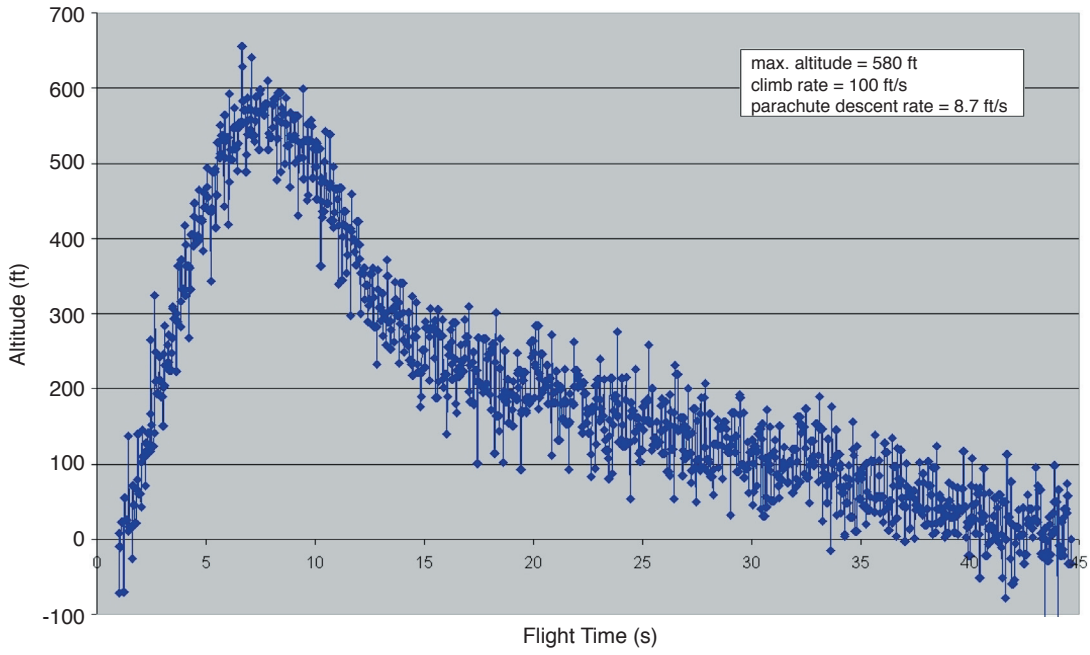

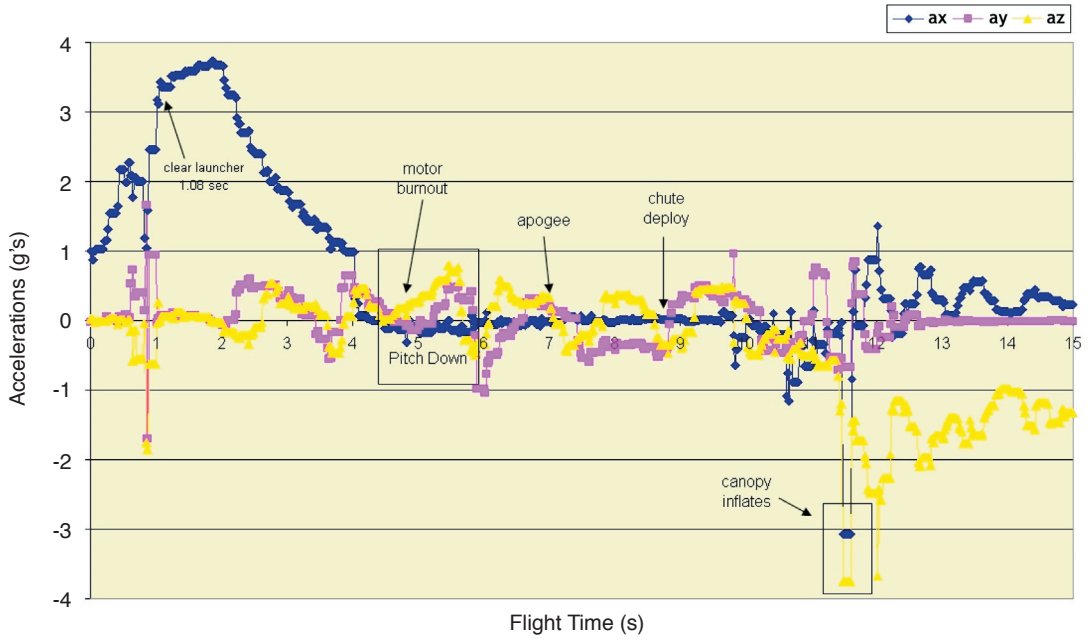

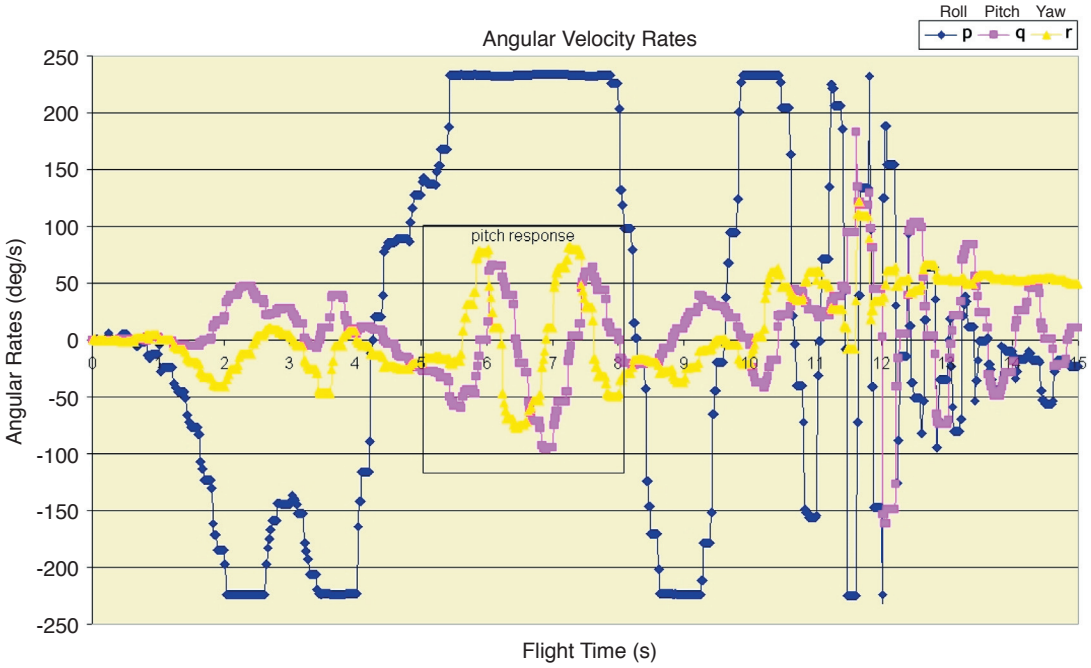
Angular Velocity Rates
Roll Pitch Yaw
p q r
pitch response
Angular Rates (deg/s)
Flight Time (s)

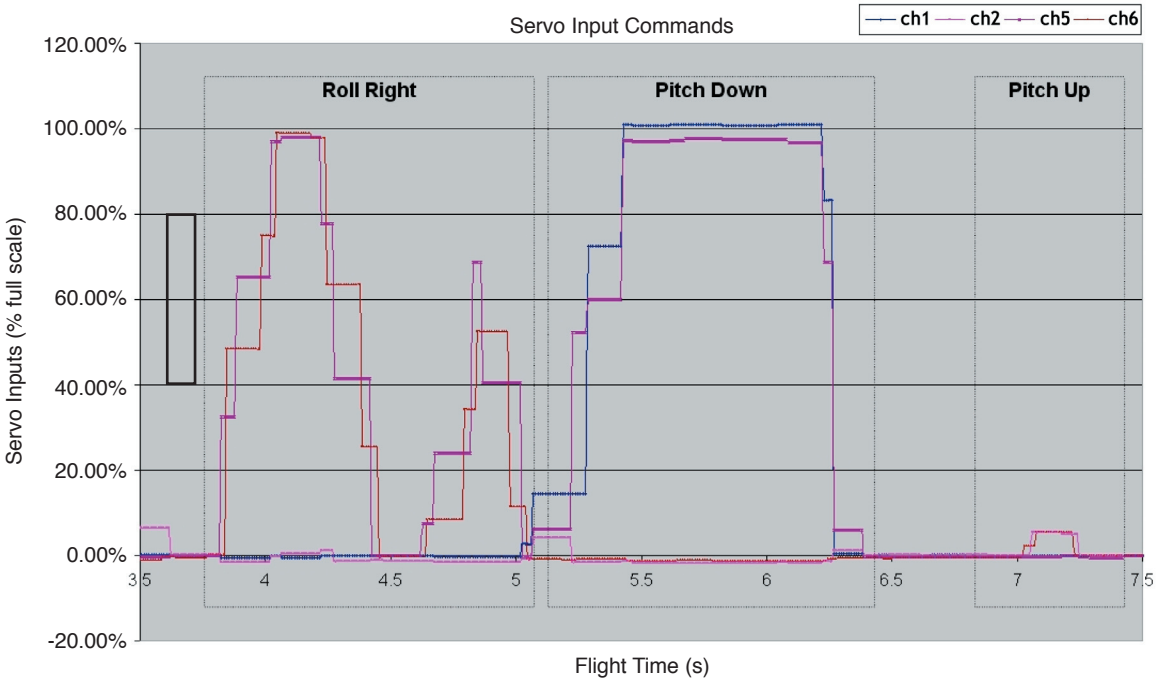
Servo Input Commands
ch1 ch2 ch5 ch6
Roll Right
Pitch Down
Pitch Up
Servo Inputs (% full scale)
Flight Time (s)